Neurobiology of Disease

HIV-1 Tat C Modulates Expression of miRNA-101 to Suppress VE-Cadherin in Human Brain Microvascular Endothelial Cells

Ritu Mishra and Sunit Kumar Singh

Laboratory of Neurovirology and Inflammation Biology, Council of Scientific and Industrial Research–Centre for Cellular and Molecular Biology, Hyderabad-500007, India

HIV-1 infection leads to the development of HIV-associated neurological disorders. The HIV-1 Tat protein has been reported to exert an adverse effect on blood–brain barrier integrity and permeability. Perturbation in permeability is mainly caused by disruptions in adherens junctions and tight junction proteins. We have identified HIV-1 Tat C-induced disruption of VE-cadherin mediated by miRNA-101 in human brain microvascular endothelial cells (BMVECs). HIV-1 Tat C increased the expression of miR-101, which led to down-regulation of VE-cadherin. Overexpression of miR-101 resulted into the suppression of VE-cadherin. Inhibition of miR-101 by the miRNA inhibitor enhanced the expression of VE-cadherin. We have demonstrated that VE-cadherin is a direct target of miR-101 using a luciferase reporter assay, which showed that mutated VE-cadherin 3′UTR and miR-101 cotransfection did not change luciferase activity. By overexpression and knockdown of miR-101, we have demonstrated that the expression level of claudin-5 is governed by the expression of VE-cadherin. These findings demonstrate a novel mechanism for the regulation of barrier permeability by miR-101 via posttranscriptional regulation of VE-cadherin in human BMVECs exposed to the HIV-1 Tat C protein.

Introduction

The CNS is protected by the blood–brain barrier (BBB) and the blood-CSF barrier (Miller et al., 2012). The BBB is composed of human brain microvascular endothelial cells (BMVECs) supported by astrocytic end feet and pericytes (Reese and Karnovsky, 1967). The barrier properties of BMVECs are due to tight junction proteins (TJPs) and adherens junction proteins (AJPs) (Dejana et al., 2008).

VE-cadherin, an endothelial cell-specific transmembrane AJP, has been reported to be a master regulator of endothelial cell–cell adhesive interactions (Lampugnani et al., 1992). TJPs mainly include claudins, occludins, and zona occludens (ZO). VE-cadherin interacts with several signaling partners to coordinate endothelial growth, TJ organization, and permeability (Dejana and Giampietro, 2012). Therefore, VE-cadherin is an important protein for the establishment and maintenance of endothelial barrier integrity (Harris and Nelson, 2010).

HIV-1 crosses the BBB during the early course of infection and infects resident brain macrophages/microglia (González-Scarano and Martin-Garcia, 2005; Persidsky et al., 2006). HIV-1 Tat protein secretes out extracellularly from the productively infected cells and affects BMVECs adversely (Westendorp et al., 1995; Xiao et al., 2000; Strazza et al., 2011). Previous studies have shown the altered expression of TJ/AJ proteins in endothelial cells caused by the HIV-1 Tat protein (Mahajan et al., 2008; Zhong et al., 2008; Gandhi et al., 2009); however, the exact mechanisms involved in this alteration are not well understood (Xu et al., 2011). In total HIV-1 infections, clade C alone infects >56% patients (Geretti, 2006). The clade-specific differences of HIV-1 Tat proteins were reflected in the differential induction of cytokines and chemokines (Gandhi et al., 2009), including differential suppression of IL-10 expression in monocytes (Wong et al., 2010). In human primary astrocytes, the expression and function of indoleamine-2,3-dioxygenase and the generation of the neurotoxin kynurenine are known to be modulated differently by clade B and C Tat proteins (Samikkannu et al., 2009). The differential roles of clade B and C Tat proteins have been highlighted in HIV-associated neurological disorders (Gandhi et al., 2010).

miRNAs are small RNA sequences 19–24 nucleotides in length that are reported to regulate ~60% of the genes in the human genome (Bartel, 2009), mostly by binding through complementary binding sites located primarily at the 3′UTR of mRNAs. The HIV-1 Tat protein has been reported to modulate the expression pattern of cellular miRNAs in neuronal cells (Eletto et al., 2008). Recently, we have also reported that the

Received Oct. 10, 2012; revised Dec. 23, 2012; accepted Feb. 6, 2013.

Author contributions: R.M. and S.K.S. designed research; R.M. performed research; R.M. and S.K.S. analyzed data; S.K.S. wrote the paper.

This work was supported by the DBT Grant BT/PR10709/AGR/36/598/2008 and by the National Institutes of Health-sponsored AIDS international Training Programme. We thank Prof. Joan W Berman (Department of Pathology, Albert Einstein College of Medicine, New York) for support, help, and valuable suggestions and the kind gift of BMVECs for this study, Mr. Manish K. Johri for construction of the pET-21b-Tat B clone, Prof. Udaykumar Ranga (Jawaharlal Nehru Centre for Advanced Scientific Research, Bangalore, India) for assistance, and the director of the Centre for Cellular and Molecular Biology for assistance in the completion of this study.

The authors declare no competing financial interests.

Correspondence should be addressed to Sunit K. Singh, PhD, New R&D Building, 1st Floor, Centre for Cellular and Molecular Biology (CCMB), Uppal Road, Hyderabad-500007, A.P., India. E-mail: sunitsingh@ccmb.res.in or sunitsingh2000@gmail.com.

DOI:10.1523/JNEUROSCI.4796-12.2013

 0270-6474/13/335992-09$15.00/0

HIV-1 Tat protein induces the expression level of miRNA-32 in human microglial cells and subsequently modulates the expression level of TRAF3 adaptor protein in microglial cells (Mishra et al., 2012). To determine the role of the HIV-1 Tat protein as a helper of HIV-1 in its process of neuroinvasion, we investigated the perturbation of miRNA in BMVECs by the HIV-1 Tat C protein. We have identified the downregulation of VE-cadherin, the master regulator of brain endothelial permeability, as a result of upregulation of miR-101 in response to HIV-1 Tat C.

Materials and Methods

Cell culture. Human brain primary microvascular endothelial cells (BMVECs) were obtained from Dr. Joan Berman (Department of pathology, Albert Einstein College of Medicine, New York) as a kind gift. BMVECs were grown in M199 medium supplemented with human endothelial growth factor (#E07600; Sigma), bovine brain serum, human serum, newborn calf serum, ascorbic acid, heparin sulfate, and glutamine (Invitrogen). BMVECs were grown in culture flasks, coverslips, and polytetrafluoroethylene (PTFE) membranes coated with 0.2% gelatin. For dose-dependent assays and time point studies, BMVECs were seeded at a 1×10^5 cell density in six-well culture dishes and incubated for 48–72 h to achieve the optimal confluency. For the luciferase assay, HeLa cells were grown in DMEM (#12100–046; Invitrogen) supplemented with 10% fetal bovine serum, 100 U of penicillin, and 100 μg/ml streptomycin (#10378016; Invitrogen). For the transactivation assay, CEM-GFP cells (obtained from the NIH AIDS Research and Reference Reagent Program) were grown in RPMI 1640 (#23400-021; Invitrogen) supplemented with 10% fetal bovine serum (#16000-044; Invitrogen), 2 mM glutamine, and 100 U/ml penicillin/streptomycin. Cultures were maintained at 37°C in a humidified chamber with a constant supply of 5% CO_2.

Expression and purification of HIV Tat protein. HIV-1 Tat C protein was expressed and purified as per our standardized protocol described previously (Mishra et al., 2012). The identity of recombinant Tat proteins was determined by Western blot analysis using anti-Tat antibody (#4138; NIH AIDS Research and Reference Reagent Program). Finally, recombinant Tat C Protein was assayed for the endotoxin level using the limulus amebocyte lysate assay (#50-647 U; Lonza) as per the manufacturer's protocol and was found to be 0.04 EU/μg of protein preparation, much below the acceptable limit of endotoxin level (1 EU/ μg of protein). To confirm the biological activity of the recombinant Tat protein, we performed a transactivation assay as described previously (Mishra et al., 2012). CEM-GFP cells (#3655; NIH AIDS Research and Reference Reagent Program); containing a stably integrated GFP gene under the control of subtype-B LTR were used for transactivation assay. Purified Tat C protein (5 μg/ml) was transfected with the ProteoJuice Protein Transfection Reagent (71281-3; Novagen), followed by visualization of GFP expressions under a fluorescence microscope (Axio Observer-A1; Carl Zeiss) after 24 h of transfection.

microRNA targets predictions. Bioinformatic prediction tools (Pictar, Target Scan 5.2, and MicroRNA.org) were used to identify the potential targets of miR-101. The target binding sites of miR-101 were found in the 3′UTR of VE-cadherin (human CDH5) transcripts using bioinformatics-based target prediction tools.

Tat treatment on BMVECs. In most of the assays, Tat C had been exposed to BMVECs at 500 ng/ml, a concentration chosen because of its closeness to the reported serum level of Tat protein that BMVECs would normally encounter in AIDS patients (Westendorp et al., 1995; Poggi et al., 2004) Human BMVECs were grown to confluency and exposed to HIV-1 Tat C protein at various doses (100, 200, and 500 ng/ml, 1 μg/ml, and 1.5 μg/ml) in serum-free media. Control cells were treated with the Tat buffer (elution buffer/storage buffer of Tat protein). BMVECs were exposed to heat-inactivated Tat C (HI-Tat C; produced by heating at 85°C for 30 min) as a control. After 12 h of HI-Tat C protein exposure, BMVECs were harvested for extraction of RNA and protein.

RNA isolation and miRNA assay. RNA isolation was done with miRNeasy kit (#217004; Qiagen). cDNA synthesis for miRNA was done with miRNA-specific primers using the TaqMan reverse transcription kit (#4366596; Applied Biosystems). Thermal incubations were as follows; 16°C for 30 min, 42°C for 30 min, and 85°C for 5 min. miRNA assays were done by quantitative PCR (qPCR) using miRNA-specific TaqMan probes and the universal PCR master mix (#4324018; Applied Biosystems). Thermal cycles were 95°C for 10 min, followed by 40 cycles of 95°C for 15 s and 60°C for 60 s. The thermal cycler ABI 7900 was used for all quantitative real-time PCR experiments.

Reverse transcription and real-time PCR. RNA was treated with DNase (#M0303L; New England Biolabs) for 30 min at 37°C. cDNA synthesis was done with Superscript II (#11904-18; Invitrogen) as per the manufacturer's protocol. Thermal incubations were as follows: 65°C for 5 min, 25°C for 10 min, 42°C for 50 min, 70° for 10 min, and, finally, RNase H treatment for 20 min at 37°C. TaqMan assays were used for the detection of VE-cadherin transcripts (#Hs00901463; Applied Biosystems).

Cell lysates and Western blot analysis. RIPA buffer (150 mM NaCl, 50 mM Tris-HCl, pH 7.5, 1% NP-40, 0.5% sodium doxycholate, 0.1% SDS, and 1× protease inhibitor mixture) was used for cell lysis. Protein concentrations were determined with the Bradford assay (#500-0006; Bio-Rad). Equal amounts of proteins were separated on 12% SDS gel and transferred on PVDF membrane at 100 V for 2 h. Membranes were blocked in 5% skim milk powder prepared in TBS–Tween 20 (TBST) buffer. Membranes were incubated overnight at 4°C with primary antibody (1:1000). After 3 washes of 10 min each with TBST, HRP-conjugated secondary antibodies were applied for 45 min. Membranes were again washed in TBST for 3 times and developed by using Super-Signal developing reagent (#34095; Pierce). Antibodies against VE-cadherin (#ab76428; Abcam), anti-claudin-5 (#34-1600; Invitrogen), anti-ZO-1 (#61-7300; Invitrogen), anti-occludin (#33-1520; Invitrogen), anti-β-tubulin (#ab6046; Abcam), anti-Dicer (#ab14601; Abcam), anti-Drosha (#ab12286; Abcam), anti-TRBP (#ab42018; Abcam), and anti-Ago2 (#ab57113; Abcam) were used in this study.

miRNA overexpression. Before 1 d of the transfection experiment, BMVECs were seeded in six-well plates at 60% confluency. Transfection mixtures were prepared in Opti-MEM (#11058-021; Invitrogen) and cells were kept in antibiotic-free media during transfection. miR-101 was overexpressed by transfecting the miRNA expression plasmid (#SC400719; Origene) with Lipofectamine 2000 (#11668-019; Invitrogen). Empty vector was used as a vehicle control. pCMV-mir-29b and scramble miR-101 were transfected into BMVECs as nonspecific controls. miR-101 overexpression was confirmed by qPCR using TaqMan probes specific to miR-101.

Anti-miR (miRNA inhibitor) transfection. BMVECs were transfected with 100 picomoles of anti-miR-101 (#AM11414; Ambion) and Cy3-labeled control anti-miR (#AM17011; Ambion) with Lipofectamine 2000. Cells were pelleted for RNA isolation and protein lysate preparation after 48 h of transfection. Transfection efficiency was monitored by visualizing the fluorescence of Cy3-labeled control anti-miR. Knockdown of miR-101 in anti-miR-transfected cells was confirmed by miR-101 assay. VE-cadherin protein expression was analyzed in BMVECs transfected with anti-miR-101 by Western blotting with anti-VE-cadherin antibody.

Luciferase reporter assay. HeLa cells were seeded in six-well plates and cotransfected with luciferase reporter clones of CDH5 3′UTR and miR-101-expressing plasmid using Lipofectamine 2000. The CDH5 3′UTR construct in pMirTarget (#HmiT000052-MT01; GeneCopeia) and miR-101 construct as pCMV-Mir (#SC400013; Origene) were used in this assay. Complementary base sequences, CATGAC, from position 1566 to 1571 of the CDH5 3′UTR were deleted to abrogate the complementary binding between miR-101 and the VE-cadherin 3′UTR. A site-directed mutagenesis kit (#200518; Stratagene) was used for generating the deletion mutations. Both the wild-type (WT) and mutant (MUT) 3′UTRs of CDH5 were transfected along with miR-101 expression clones in HeLa cells. Cells were harvested for luciferase assays after 24 h of transfection. Luciferase assays were performed with a luciferase assay kit (#E4030; Promega) according to the manufacturer's protocol. The β-galactosidase assay (#E2000; Promega) was used for normalization.

Transendothelial electrical resistance assay. A 3.0 μm pore PTFE membrane insert (12-well plate; #3494; Corning Life Sciences) was used in the permeability assays. EVOM2 (World Precision Instruments) was used to

read the electrical resistance in all experiments. Insert membranes were precoated with 0.2% gelatin followed by cell seeding at a density of 2×10^4 in 500 μl of complete media in the upper chamber of a Transwell membrane. Additional gelatin coating over membrane inserts was found to be more helpful in optimal adherence of BMVECs rather than direct seeding of cells on collagen-coated surfaces. Transendothelial electrical resistance (TEER) values were monitored until the BMVECs reached optimal confluency (~4–6 d). When TEER values became quite stable and were not showing any further increase, monolayers were considered as a confluent layer. Once BMVECs reached confluency in a monolayer, they were treated with different doses of Tat C protein and TEER was recorded after 12 h. TEER of BMVECs was recorded at different time points in a time course experiment.

Fluorescence permeability assay. BMVECs were seeded on a 3.0 μm pore PTFE membrane insert similar to that described for the TEER assay. BMVECs were treated with different doses of Tat proteins and, after 12 h of treatment, cells were washed with HBSS buffer and incubated with 0.005% water-soluble sodium fluorescein (molecular weight 376.28; #064738; Survival Research Laboratories) solution in the upper chamber of the insert membrane. After 30 min of incubation at 37°C, 100 μl of the solution was collected from the lower chamber of wells and assayed for the fluorescence at 480/530 nm wavelength (Infinite M200; Tecon).

Statistical analysis. Data are expressed as the mean ± SEM from three independent biologically repeated experiments. $p < 0.05$ was considered as significant in a one-tailed array. Comparison of the treated group versus the untreated group was analyzed with Student's *t* test. For the miR-101 assay, results are presented as the fold change relative to controls.

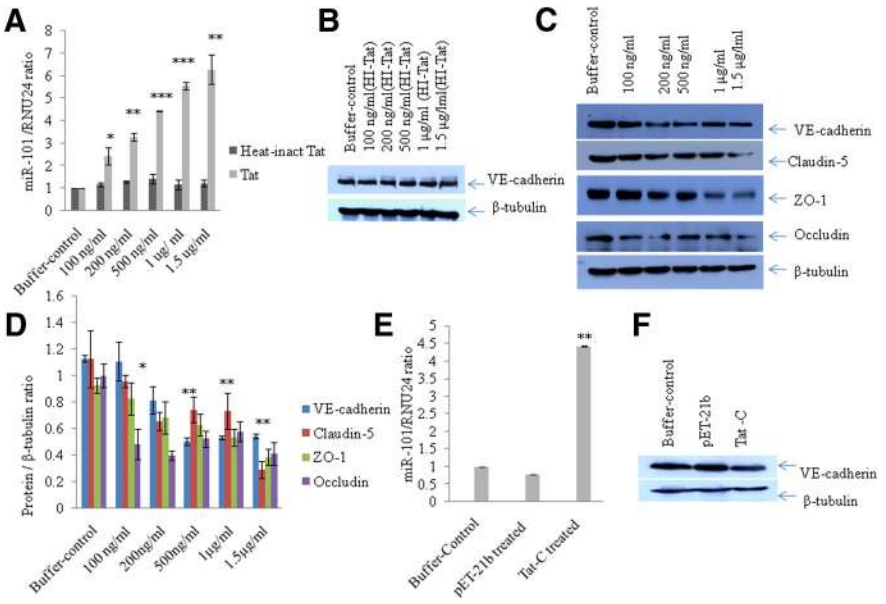

Figure 1. Expression of VE-cadherin and other TJPs decreases upon Tat C treatment in a dose-dependent manner. ***A***, Fold change in miR-101 expression level after treatment with increasing doses of HIV-1 Tat C protein and HI-Tat C in BMVECs. BMVECs were harvested for protein and RNA analysis after 12 h of Tat C treatment. Expression of miR-101 was determined by qPCR using the human miR-101-specific TaqMan assay. The expression level of a small RNA, RNU24, was used as a normalizer. Results are shown as the fold change compared with control. Changes in the expression levels of miR-101 are statistically significant. $*p \leq 0.05$; $**p \leq 0.005$; $***p \leq 0.0005$. ***B***, Western blot analysis demonstrating no change in the VE-cadherin expression level in BMVECs after exposure to the HI-Tat C protein. ***C***, Western blots analysis for VE-cadherin and other TJPs (claudin-5, ZO-1, occludin) of samples treated with increasing doses of Tat C showing a decrease at the protein expression level. ***D***, Graph showing densitometry analysis of the results. Image density of Western blots has been normalized with β-tubulin using ImageJ software. Changes in TJPs and VE-cadherin in BMVECs exposed to the Tat C protein are statistically significant. $**p \leq 0.005$; $*p \leq 0.05$. For ZO-1, $*p \leq 0.05$ at all doses; at 1.5 μg/ml Tat C treatment, $**p \leq 0.005$. For occludin, downregulation is statistically significant at all doses of Tat C, $*p \leq 0.05$; at 1.5 μg/ml Tat C treatment, $**p \leq 0.005$. Downregulation of claudin-5 was statistically significant. $*p \leq 0.05$. Results are representative of three biologically repeated experiments and are represented as mean ± SE. ***E***, Fold change in miR-101 expression level in BMVECs after Tat C treatment and empty vector pET-21b purified in a similar manner, showing that upregulation of miR-101 is specific to Tat C. ***F***, Western blot analysis of the pET-21b and Tat C-treated BMVECs showing that downregulation of VE-cadherin is specific to Tat C and is not induced by either buffer or empty vector. All experiments were repeated three times and are represented as mean ± SE.

Results

miR-101 expression level increases upon HIV-1 Tat C treatment in human BMVECs

We reported previously that HIV-1 Tat C is able to induce the cellular level of certain miRNAs in human microglial cells (Mishra et al., 2012). Based on the available data about the role of the HIV-1 Tat protein in the modulation of cellular miRNAs, we hypothesized that there might be perturbations in miRNA expression patterns in BMVECs upon HIV-1 Tat exposure. In the present study, we investigated the expression level of miR-101 in the Tat C-treated BMVECs to search for any perturbation due to the HIV-1 Tat C protein. Interestingly, the expression level of miR-101 in BMVECs showed a significant upregulation ($p \leq 0.005$) after Tat C exposure in a dose-dependent manner (Figure 1*A*). The expression level of miR-101 was ~2.5-fold higher compared with control cells when exposed to 100 ng/ml Tat C protein and this increase was linear, as shown in Figure 1*A*. To determine the specificity of the HIV-1 Tat C protein for induction of miR-101, we also investigated the level of miR-101 in BMVECs treated with the pET-21b empty-vector-eluted fraction, as well as with the HI-Tat C protein. The eluted empty vector pET-21b did not result in the upregulation of miR-101 (Fig. 1*E*). Similarly, HI-Tat C protein treatment of BMVECs did not affect the expression of miR-101 in dose-dependent manner (Fig. 1*A*).

HIV-1 Tat C exposure to BMVECs suppresses the expression of VE-cadherin and other TJPs

To study the effects of HIV-1 Tat C on BMVECs, we determined the expression levels of various TJPs (Claudin-5, ZO-1, occludin) and the major AJP VE-cadherin. We found a significant decrease in the expression of VE-cadherin and TJPs (Claudin-5, ZO-1, occludin) at the protein level in BMVECs exposed to Tat C in a dose-dependent manner (Fig. 1*B*). The downregulation of VE-cadherin was totally abrogated when BMVECs were treated with HI-Tat C protein in similar doses (Fig. 1*B*). Treatment of BMVECs with empty pET-21b vector did not affect the expression of VE-cadherin (Fig. 1*F*). Not just increasing the dose of Tat C, but also the extended duration of exposure (2, 6, 12, and 24 h) of Tat C to BMVECs also resulted in a significant decrease in the expression level of AJP and VE-cadherin (Fig. 2*A*,*B*). In another experiment, BMVECs were exposed to Tat B protein, and the VE-cadherin expression level did not decrease significantly compared with that of the Tat C protein (Fig. 3*D*). Remarkably, miR-101 was not upregulated in the BMVECs exposed to HIV Tat-B protein (Fig. 3*C*). These findings suggest that the regulation of VE-

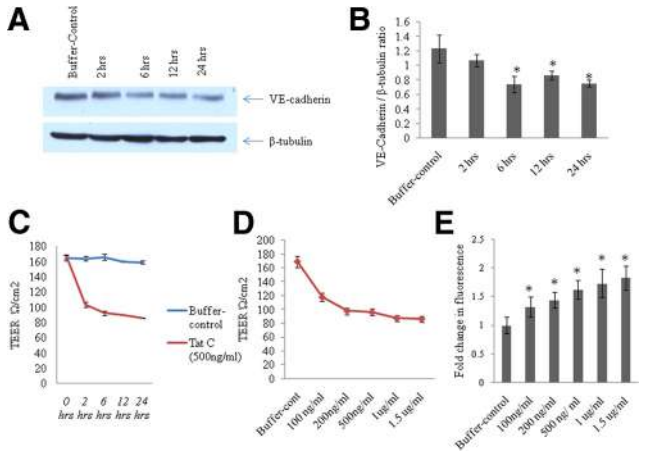

Figure 2. Decrease in expression of VE-cadherin and TEER with extended exposure of Tat C to BMVECs and disruption of endothelial barrier function. ***A***, Western blot analysis showing decrease in the expression level of VE-cadherin in BMVECs with the increase in time of exposure of Tat C (500 ng/ml) to BMVECs. ***B***, Graph representative of three independent experiments showing a decrease in VE-cadherin expression with the increase in time of exposure of Tat C (500 ng/ml) to BMVECs. The VE-cadherin expression level started decreasing significantly after 6 h ($p \leq 0.05$). ***C***, Graph showing the decrease in TEER value with the increase in time of exposure of Tat C (500 ng/ml) to BMVECs. Increase in the time of exposure of the Tat C protein on BMVECs disrupted the barrier integrity of BMVECs and thereby increased the permeability ($p \leq 0.005$). ***D***, Graph showing the dose-dependent decrease in the TEER value after Tat C treatment. ***E***, Bars indicating the fold changes in fluorescence after leakage of fluorescent compound (sodium fluorescein) across the monolayer of BMVECs exposed to Tat C protein ($p \leq 0.05$). The migration of sodium fluorescein through control cells was set at 1 and the results are shown accordingly. As the dose of Tat C is increasing, the migration of sodium fluorescein is increasing from upper compartment to the lower compartment of the Transwell insert membrane culture experiment. All experiments were repeated three times and are represented as mean ± SE.

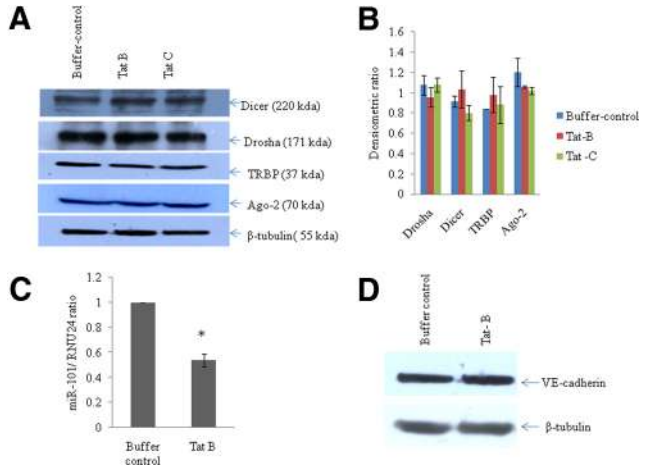

Figure 3. No significant effect of HIV-1 Tat B or Tat C on the expression of major miRNA biogenesis pathway proteins. ***A***, Western blot analysis for tracking the changes in expression level (if any) of major proteins involved in miRNA biogenesis. BMVECs were exposed for 12 h to Tat B and Tat C proteins (500 ng/ml) and cells were harvested and tested for major proteins (Drosha, Dicer, Ago-2, TRBP). Neither clade of HIV-1 Tat protein (Tat B and Tat C) could exert any significant change in the expression of Drosha, Dicer, Ago-2, or TRBP. ***B***, Densitometry quantitation of Drosha, Dicer, TRBP, and Ago-2 proteins as normalized with image density of β-tubulin by using ImageJ software. Results are representative of three independent biological repeats and are shown as mean ± SE. No significant change can be seen ($p \geq 0.05$). ***C***, Bar diagram showing downregulation of miR-101 in BMVECs exposed to the Tat B protein. The expression level of miR-101 was quantified by specific TaqMan probes using RNU24 as a normalizer. ***D***, Western blot analysis of VE-cadherin in Tat B-treated BMVECs demonstrates the differential regulation of VE-cadherin expression. All experiments were repeated three times and are represented as mean ± SE.

cadherin in BMVECs is mediated posttranscriptionally by miR-101 induced by the HIV-1 Tat C protein.

HIV-1 Tat C treatment exerts endothelial barrier dysfunction

Given the major role of AJPs and TJPs in the maintenance of barrier integrity in BMVECs, we also investigated the effect of the HIV-1 Tat C protein on barrier permeability. BMVECs grown on the insert membrane were treated with Tat C protein (100 ng to 1.5 μg) for the dose-dependent experiment and for the time points 2–24 h for the time course experiment, as described in the Materials and Methods. Tat C treatment resulted into a significant ($p \leq 0.005$) decrease in TEER values for all doses of Tat C protein exposed to the BMVECs (Fig. 2*D*). TEER values also decreased significantly when measured at different exposure times (Fig. 2*C*). These results indicated that the downregulation of VE-cadherin and other TJPs (Fig. 1*C*,*D*, Fig. 2*A*,*B*) due to HIV-1 Tat C treatment is responsible for the barrier disruption in BMVECs shown as decreased resistance across the endothelial monolayer. Leakage of a fluorescent substance (sodium fluorescein) was also used as a standard for determining the BMVEC permeability in this study. The migration of sodium fluorescein increased with the increase in the dose of Tat C exposure to BMVECs (Fig. 2*E*).

HIV-1 Tat C does not regulate miRNA biogenesis machinery

Virus and viral products are known to modulate the cellular RNAi machinery in various ways (Santhakumar et al., 2010). To study whether the perturbation in the expression level of miR-101 in BMVECs exposed to the HIV-1 Tat C protein is associated with any alteration in the miRNA biogenesis machinery, we determined the expression level of major proteins (Drosha, Dicer, Ago2, and TRBP) involved in miRNA biogenesis. In BMVECs exposed to HIV-1 Tat C and Tat B, we could not find any substantial change in the expression of these proteins (Fig. 3*A*,*B*). This observation indicated that the HIV-Tat protein does not modulate the expression of major proteins involved in miRNA biogenesis machinery in BMVECs.

miR-101 targets the 3′UTR of VE-cadherin directly

miR-101 was induced in BMVECs exposed to the HIV-1 Tat C protein (Fig. 1*A*). To identify the effect of miRNA-mediated posttranscriptional regulation of miR-101 in BMVEC permeability; we searched for potential targets of miR-101 using bioinformatics prediction tools (Targetscan 5.2, Pictar, and Miranda), which showed strong and multiple binding sites for miR-101 in the 3′UTR of VE-cadherin (also referred to as CDH5 3′UTR). As shown in Figure 1*A*, the dose-dependent increase in the expression of miR-101 after Tat C treatment and the concordant decrease in the expression level of VE-cadherin suggests that the expression level of VE-cadherin might be regulated by miR-101 (Fig. 4*A*). VE-cadherin 3′UTR is one of the longest 3′UTRs, which introduced the strong possibility of its posttranscriptional regulation being mediated by miRNAs. We used a luciferase reporter assay to determine whether miR-101 binds the VE-cadherin 3′UTR directly. The construct encompassing firefly luciferase reporter followed by the full-length 3′UTR of VE-cadherin was used. Expression constructs for miR-101, miR-29b, and empty vector were cotransfected with the VE-cadherin 3′UTR reporter into HeLa cells. The mutant 3′UTR construct of VE-cadherin (having deletion in binding sites complementary to miR-101; Fig. 4*A*) was also transfected to determine the specificity of the binding of miR-101 with the cadherin 3′UTR. Luciferase activity was diminished by almost 65% after

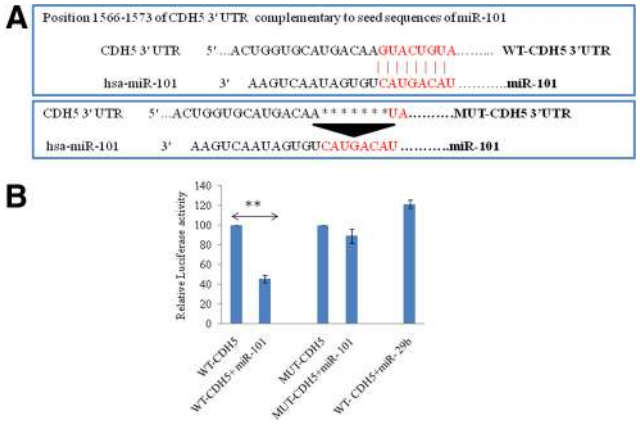

Figure 4. miR-101 binds complementary sequences in CDH5 3′UTR directly and regulates the expression of CDH5 (VE-cadherin). ***A***, Schematic representation of seed sequences in miR-101 and complementary 8-mer binding sites in WT-CDH5 3′UTR (VE-cadherin).The complementary sites are deleted in MUT-CDH53′UTR using a site-directed mutagenesis kit to abrogate the regulatory interaction of miR-101 in the 3′UTR of CDH5. WT and MUT-CDH5 3′UTR reporter constructs were cotransfected with miR-101, miR-29b, and pCMV-β-gal (as a normalizing control) plasmids and luciferase assays were performed in the HeLa cells. ***B***, miR-101 transfection suppressed the luciferase activity significantly ($p \leq 0.005$) in the WT-CDH5 3′UTR cotransfection. miR-101 transfection could not represse the luciferase activity when cotransfected with the MUT-CDH5 3′UTR. An irrelevant miR-29b, which does not have the complementary sequences for CDH5 3′UTR, did not perturb the luciferase activity. The luciferase expression level of cells (transfected with only 3′UTR of VE-cadherin) was considered as a control with 100% relative light unit and the results are shown accordingly. All experiments were repeated three times and are represented as mean ± SE. $^{**}p \leq 0.005$.

cotransfection of the VE-cadherin 3′UTR and miR-101 ($p \leq 0.005$; Fig. 4*B*). The mutant 3′UTR construct of VE-cadherin (Fig. 4*A*) devoid of complementary sequences for miR-101 did not show significant reduction in luciferase activity (Fig. 4*B*). The cotransfection of 3′UTR of VE-cadherin and an irrelevant miR-29b expression construct also did not show any decrease in the luciferase activity (Fig. 4*B*).

miR-101 overexpression downregulates cellular VE-cadherin expression level

After confirming the site-specific complementary binding between miR-101 and VE-cadherin 3′UTR, we investigated the effect of miR-101 at the protein expression level of VE-cadherin in BMVECs. A P-CMV-miR-101 construct encoding miR-101 was transfected in BMVECs, and the overexpression of miR 101 was confirmed by determining the level of expression of miR-101 using the TaqMan assay. After 24 h of transfection, the level of expression of miR-101 was nearly 8.5-fold higher (Fig. 5*A*; $p < 0.05$). Overexpression of miR-101 resulted into a 45% reduction of VE-cadherin expression at the protein level (Fig. 5*B*,*C*). The specificity of regulation was determined by transfecting another irrelevant miRNA, miR-29b (Fig. 5*B*,*D*). This miRNA was not able to suppress the expression level of VE-cadherin in BMVECs (Fig. 5*B*,*C*). The reduction was also evident at the mRNA level of VE-cadherin in miR-101-transfected cells (Fig. 5*D*). These results demonstrated that the cellular expression level of miR-101 has an important role in the translational regulation of VE-cadherin. As a proof of concept, the scramble miR-101 was also transfected in BMVECs at 100 and 200 pmol concentrations. The scramble miR-101 sequence did not bring about any change in the expression level of VE-cadherin (Fig. 5*F*).

Anti-miR-101 rescues the expression level of VE-cadherin in the presence of HIV-1 Tat C protein

The objective of this experiment was to determine both the regulatory effect of miR-101 on VE-cadherin expression and to determine the rescuing ability of anti-miR-101 in preserving the expression level of VE-cadherin even in the presence of HIV-1 Tat C, which has been shown to suppress VE-cadherin and thereby the permeability of BMVECs. To confirm the direct regulation of expression of VE-cadherin by miR-101, we tranfected the BMVECs with the miRNA inhibitor of miR-101, here referred to as anti-miR-101. After transfection of anti-miR-101, BMVECs were exposed to the HIV-1 Tat C protein. Cy3-labeled scramble anti-miR was used to test the transfection efficiency and as a negative control. The cellular miR-101 levels were quantified using qPCR to confirm the modulation of miR-101 as per the experimental design (Fig. 6*A*). The stand-alone transfection of anti-miR-101 in BMVECs was found to upregulate the expression level of VE-cadherin significantly (Fig. 6*B*; $p \leq 0.05$). However, when the miR-101-transfected cells were additionally treated with the HIV-1 Tat C protein, there was a significant regain of VE-cadherin expression (Fig. 6*B*,*C*; $p \leq 0.05$), indicating that anti-miR-101 was able to nullify the suppressive effect of Tat C on the expression of VE-cadherin mediated by miR-101.

Expression level of VE-cadherin influences the expression level of Claudin-5 directly

VE-cadherin and claudin-5 represent the key components of the AJs and TJs, respectively (Nitta et al., 2003). HIV-1 Tat C exposure to BMVECs showed a gradual, dose-dependent decrease in the expression levels of both proteins (Fig. 1*B*) and a decrease in the permeability of BMVECs (Fig. 2*D*). The expression level of claudin-5 was also monitored in the experimental setups using overexpression of miR-101 and anti-miR-101 transfection, in which we had already showed that the regulation of VE-cadherin expression is mediated by miR-101. The rationale behind these experiments was to demonstrate the regulatory role of VE-cadherin over claudin-5 in BMVECs. The upstream regulatory role of VE-cadherin on claudin-5 has also been reported previously (Taddei et al., 2008). A regulatory role of VE-cadherin on claudin-5 suggested that VE-cadherin might play a central role in maintaining the endothelial cell lineage, which was again supported by the fact that claudin-5 expression is limited to the VE-cadherin-expressing cells (Gavard and Gutkind, 2008).

In all experiments, we observed a trend showing a regulatory role of VE-cadherin on claudin-5 (Fig. 7*A*). Upon overexpression of miR-101, when VE-cadherin was being suppressed, we observed the same trend for claudin-5 (Fig. 7*C*). In BMVECs transfected with anti-miR-101, there was a significant regain of claudin-5 expression (Fig. 7*B*,*D*), which is consistent with the regain of VE-cadherin in anti-miR-101 transfection (Fig. 6*C*, Fig. 8). These results confirm the idea of functional hierarchy of VE-cadherin in the establishment of the endothelial cell–cell junctions.

Discussion

The BBB acts as a structural and functional barrier protecting the CNS from macroconstituents such as drugs, pathogens, and neurotoxins flowing from the periphery to the CNS and vice versa (Spudich and Ances, 2011). Many neurotropic viruses, such as HIV-1, human T-cell leukemia virus (HTLV-1), lymphocytic choriomeningitis virus (LCMV), West Nile virus (WNV), and hantaviruses, are known to disrupt the BBB via the endothelial junctions (Spindler and Hsu, 2012). HIV-1 infection in the CNS

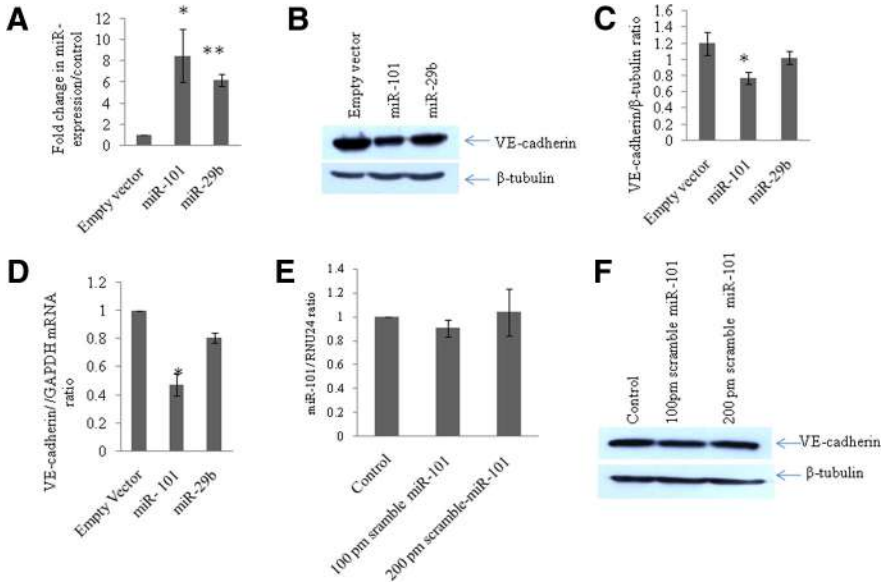

Figure 5. Overexpression of miR-101 reduces the expression of VE-cadherin in BMVECs. ***A***, Graph showing the fold change in miR-101 and miR 29b in miR-101- and miR-29b-overexpressed BMVECs, respectively, via qPCR using the TaqMan miR-101 and TaqMan miR-29b assays. The miR-101 level was found to be 8.5-fold higher in miR-101-transfected cells compared with vector control ($p \leq 0.05$). ***B***, Western blot analysis for VE-cadherin in BMVECs after overexpression of miR-101. Empty vector was used as a negative control and the plasmid pCMV-miR-29b was used as nonspecific miRNA to test the specificity of regulation. In miR-101 overexpression, the VE-cadherin expression level is downregulated significantly ($p \leq 0.05$). ***C***, Densitometry image density analysis of VE-cadherin using β-tubulin as a normalizer in ImageJ software. All experiments were repeated three times and are represented as mean ± SE. ***D***, qPCR analysis of VE-cadherin in miR-101- and miR-29b-overexpressed cells to determine changes at the transcript level. Total RNA was reverse transcribed by using random hexamers and transcript levels were quantified with VE-cadherin-specific TaqMan probes using GAPDH as an internal reference. Fold changes were determined with the $\Delta\Delta$ct method. ***E***, Fold change in miR-101 expression level after transfection of scramble miR-101in BMVECs showing no significant change. ***F***, Western blot analysis for VE-cadherin in scramble miR-101-transfected BMVECs showing no change in their protein expression level. All experiments were repeated three times and are represented as mean ± SE.

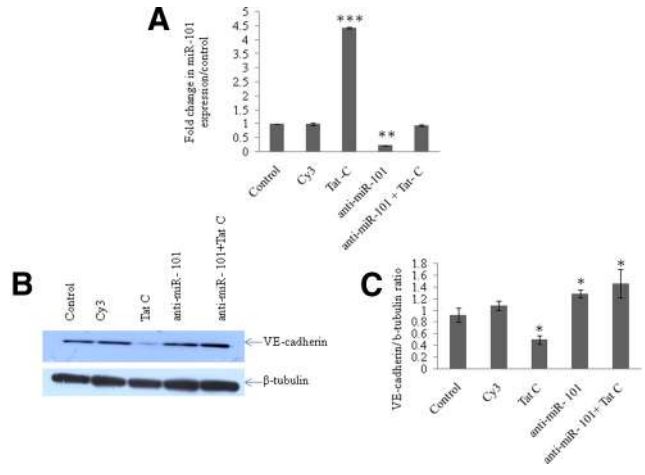

Figure 6. Anti-miR-101 transfection rescues the VE-cadherin expression level in BMVECs. ***A***, Anti-miR-101 transfection resulted in the reduced expression of miR-101. An ~80% reduction in the expression of cellular miR-101 in anti-miR-101-transfected BMVECs was seen compared with scramble-transfected negative controls. *$p \leq 0.05$. ***B***, Western blot analysis to determine the regain in level of expression of VE-cadherin in anti-miR-101-transfected BMVECs. After 24 h of anti-miR-101 transfection in BMVECs, cells were again exposed to Tat C protein (500 ng/ml) to test the specificity of the miR-101-mediated control over the expression of VE-cadherin, but the expression of VE-cadherin remained unaffected due to the suppressive effect of anti-miR-101 on miR-101 ($p \leq 0.05$). ***C***, Western blot images of VE-cadherin were normalized with β-tubulin and are presented as graph bars. All experiments were repeated three times and are represented as mean ± SE. *$p \leq 0.05$.

is reported to be an early event after primary infection (Hazleton et al., 2010), however, the mechanisms of perturbation of the BBB during HIV-1 infection are not fully understood. The HIV-1 Tat protein has been implicated in HIV neuropathogenesis and is regarded as a major player in BBB disruption (Hui et al., 2012). HIV-1 Tat has been reported as an active player in several vascular pathologies of HIV-1 in the CNS, in which HIV does not infect the cell directly, but affects the functionality in a bystander fashion (Zhong et al., 2008). The circulating Tat protein in the serum of HIV-1-infected patients has been reported to range from 300 to 550 ng/ml (Westendorp et al., 1995; Poggi et al., 2004). To mimic the conditions of this bystander effect, we performed our experiments on the primary human BMVECs by exposing them to the HIV-1 Tat C protein. We demonstrated that HIV-1 Tat C upregulates the expression levels of miR-101 in BMVECs (Fig. 1*A*), which in turn posttranscriptionally regulate the expression level of VE-cadherin. Pacifici et al. (2013) reported the induced expression of miR-101 in their miRNA expression profiling of the CSF of AIDS patients displaying the symptoms of HIV-associated encephalitis. It is known that the HIV-1 Tat protein can easily transfuse through cells (Frankel and Pabo, 1988).

We found a significant upregulation of miR-101 in BMVECs on Tat C treatment. The modulation in the expression pattern of miRNAs has been reported in other cells exposed to HIV-1 Tat. Perturbation of the presynaptic protein SNAP25 via miR-128 (Eletto et al., 2008), suppression of the CYP2E1 protein in neurons through miR-1 (Fiore et al., 2009), and the induction of miR-34a to downregulate their target genes (Chang et al., 2011) have been described previously. We have also reported previously the miR-32-mediated regulation of TRAF3 after Tat C exposure (Mishra et al., 2012). Having conserved seed sequences across the mammalian species, miR-101 seemed to have a potential role in gene regulation (John et al., 2006).

We found a dose-dependent decreased expression of a major AJP, VE-cadherin, in response to Tat C treatment. VE-cadherin has a predominant role in orchestrating the architecture of adherence junctions in endothelial cells. However, the precise mechanism for the regulation of VE-cadherin and its impact on endothelial permeability was not well understood, specifically in the case of the bystander hit of the HIV-1 Tat protein. This decrease in the expression of VE-cadherin was manifested at the level of endothelial functions in terms of the compromised permeability of the endothelial monolayer (Fig. 2*C–E*). Significant decreases in TEER value and accelerated fluorescein migration were observed even at low concentrations of Tat C (100 ng/ml), whereas the total VE-cadherin expression level did not change significantly. This might have been due to early inflammatory responses (secretion of cytokines, chemokines) in endothelial cells exposed to Tat, which could induce the internalization of

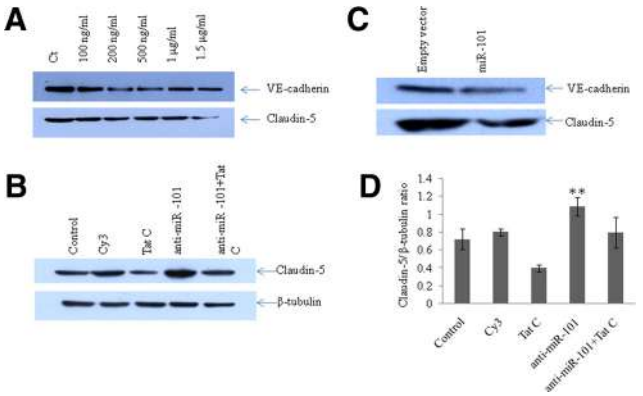

Figure 7. Expression level of VE-cadherin influences the expression level of Claudin-5 directly. To distinguish the direct effect of expression level of VE-cadherin on the expression level of claudin-5, three sets of experiments were performed. ***A***, The downregulation of VE-cadherin upon Tat C treatment decreases the expression level of claudin-5 in a dose-dependent manner. ***B***, Transfection of anti-miR-101 in BMVECs showing the same trend of rescued expression of claudin-5 as in the regained expression of VE-cadherin, even in the presence of the Tat C protein. ***C***, Overexpression of miR-101 decreases the expression level of claudin-5 in the same way as that of VE-cadherin. ***D***, Densitometry analysis using ImageJ software of Western blot images for claudin-5 in anti-miR-101 transfection experiments. A significant recovery of claudin-5 expression level can be seen ($p \leq 0.005$). All experiments were repeated three times and are represented as mean ± SE. $^{**}p \leq 0.005$.

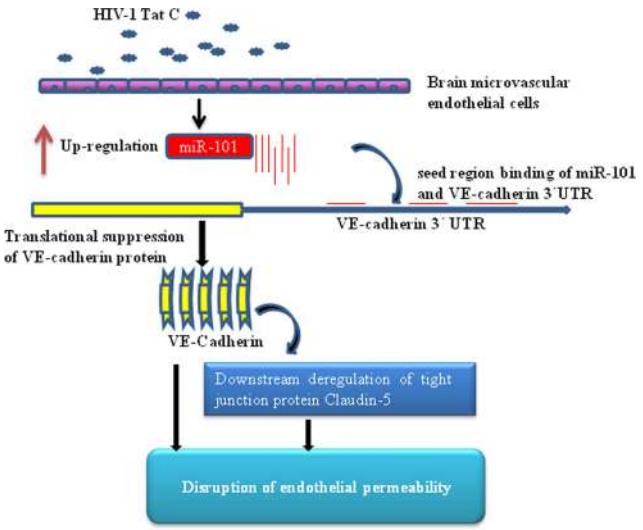

Figure 8. Proposed model for Tat C-mediated downregulation of VE-cadherin and claudin-5 in BMVECs through miR-101. We propose that expression of VE-cadherin is regulated through miR-101 in BMVECs exposed to the HIV-1 Tat C protein. After HIV-1 Tat C treatment, the expression level of miR-101 increases and targets the expression level of VE-cadherin directly, which in turn influences the expression level of claudin-5 and thereby the permeability in BMVECs.

VE-cadherin from the cell surface to the cellular compartment (Zhu et al., 2012).

Other groups have reported the disruption of TJs such as claudin-5, occludin, and ZO-1 (Zhong et al., 2008; András and Toborek, 2011; Xu et al., 2012) due to the effect of inflammatory cytokines/chemokines (Andriopoulou et al., 1999). Tat is reported to decrease occludin expression by cleaving through MMP9 (Xu et al., 2012). The downregulation of occludin and ZO-1 in brain microvessels has been reported to be due to prostaglandin E2 (Pu et al., 2007). Activation of VEGFR-2 and many other redox-regulated signal transduction pathways are thought to contribute to the Tat-mediated downregulation of claudin-5 (András et al., 2005).

In this study, we elucidated the mechanism of downregulation of VE-cadherin, the predominant AJP. VE-cadherin is located on cell–cell junctions and primarily controls the physical adherence between cell membranes, along with connecting the intercellular network of cytoplasmic proteins such as p120, β-catenin, and plakoglobin and cytoskeletal microfilaments (Dejana et al., 1999; Vincent et al., 2004; Dejana et al., 2008). The expression level of VE-cadherin has been found frequently to be altered in inflammatory conditions such as diabetes and viral infections (Alexander et al., 2000; Dewi et al., 2008). We have demonstrated previously that HIV-1 Tat C is able to upregulate the expression of miR-101, which is accompanied by a decrease of VE-cadherin in BMVECs (Fig. 1). Overexpression of miR-101 in BMVECs resulted into the decreased expression of VE-cadherin at both the protein and mRNA levels (Fig. 5*B*,*D*). This was the first indication of VE-cadherin regulation through miR-101. However, we did not observe reduced expression of VE-cadherin in the BMVECs transfected with irrelevant miR-29b (Fig. 5*B*), suggesting that the VE-cadherin regulation through miR-101 is highly specific. Scramble miR-101 was also transfected in BMVECs at 100 and 200 pmol concentrations. The cells transfected with scramble miR-101 showed perturbation in neither the expression of cellular miR-101 nor protein expression of VE-cadherin (Fig. 5*E*,*F*). This demonstrated the regulation of VE-cadherin through sequence-specific binding of seed sequences of miR-101 and 3′UTR of VE-cadherin.

To demonstrate the miRNA-mediated regulation more specifically, BMVECs were transfected with anti-miR-101. This inhibitor has the complementary sequences for the miR-101 seed region. The purpose of this transfection was to capture and restrict the expression level of cellular mature miR-101. As expected, it restrained the miR-101 level in BMVECs (Fig. 6*A*), which resulted in the elevated expression of VE-cadherin (Fig. 6*B*). This regain of VE-cadherin became more obvious when BMVECs were transfected with anti-miR-101 and exposed to HIV-1 Tat C protein. Even in the presence of Tat C, BMVECs did not show downregulation of VE-cadherin (Fig. 6*B*). This revealed the potential effect of anti-miR-101 in combating the endothelial disruption. This finding confirmed that HIV-1 Tat C-mediated upregulation of miR-101, which is nullified by presence of anti-miR-101 in transfected BMVECs, was now not able to reduce the VE-cadherin expression. This indicated that miRNA-mediated regulation may operate over and/or along with other mechanisms in the regulation of VE-cadherin in human BMVECs.

We performed a luciferase reporter assay to investigate the negative regulation of VE-cadherin by miR-101. Cotransfection of miR-101 with the 3′UTR of VE-cadherin suppressed the luciferase activity significantly ($p \leq 0.005$). The luciferase activity was restored after mutating the binding sites of miR-101 in the 3′UTR luciferase reporter construct, which established VE-cadherin as a direct target of miR-101 and explained the miR-101-mediated posttranscriptional regulation of VE-cadherin in BMVECs. Specificity of the interaction between miR-101 and VE-cadherin was again demonstrated by the cotransfection of 3′UTR reporter constructs with the irrelevant miRNA miR-29b, which did not reduce the luciferase activity (Fig. 4*B*).

The brain's endothelial permeability is the joint attribute of both TJPs and AJPs. These proteins act together for maintaining the adhesive interactions required for barrier integrity of BMVECs. We have demonstrated that the posttranscriptional regulation of VE-cadherin is mediated through miR-101 and that the expression of VE-cadherin governs the expression patterns of the TJP claudin-5 directly. In experiments related to the overexpres-

sion of miR-101 and suppression of cellular miR-101 by anti-miR-101, the expression level of claudin-5 followed the same trend as that of VE-cadherin (Fig. 7*B*,*C*). These findings are consistent with previous studies showing that the levels of VE-cadherin modulated the expression of claudin-5 directly (Taddei et al., 2008). VE-cadherin has been reported to control the transcription of claudin-5 by tethering the repressive transcription factors FoxO1 away from the claudin-5 promoter (Taddei et al., 2008). In another study, Nitta et al. (2003) reported that VE-cadherin-deficient mice were embryonically lethal compared with claudin-5 knock-out mice, which followed the course of normal development initially but died soon due to BBB dysfunction. These reports suggested that VE-cadherin plays a predominant regulatory role in the constitution of the endothelial barrier junctions in BMVECs. VE-cadherin is positioned upstream in the regulatory cascade and influences claudin-5 and the maintenance of endothelial barrier functions directly. The interactions of these two important proteins are unique to the brain barrier compared with other junctions such as epithelial cell junctions (Dejana, 2004). This master regulatory role of VE-cadherin provides another opportunity to modulate other downstream targets, playing an important role in vascular biology by shaping VE-cadherin expression in endothelial cells (Gavard and Gutkind, 2008). In the present study, we have demonstrated for the first time that HIV-1 Tat C upregulates the expression level of miR-101 in BMVECs and consequently suppresses the expression of VE-cadherin. The suppression of VE-cadherin results in the reduced expression level of claudin-5, which in turn compromises the permeability of BMVECs. This study presents a novel miRNA-mediated mechanism for the HIV-1 Tat C-induced decrease in VE-cadherin expression and subsequent dysfunctions in the barrier integrity of BMVECs.

References

Alexander JS, Alexander BC, Eppihimer LA, Goodyear N, Haque R, Davis CP, Kalogeris TJ, Carden DL, Zhu YN, Kevil CG (2000) Inflammatory mediators induce sequestration of VE-cadherin in cultured human endothelial cells. Inflammation 24:99–113. CrossRef Medline

András IE, Toborek M (2011) HIV-1-induced alterations of claudin-5 expression at the blood-brain barrier level. Methods Mol Biol 762:355–370. CrossRef Medline

András IE, Pu H, Tian J, Deli MA, Nath A, Hennig B, Toborek M (2005) Signaling mechanisms of HIV-1 Tat-induced alterations of claudin-5 expression in brain endothelial cells. J Cereb Blood Flow Metab 25: 1159–1170. CrossRef Medline

Andriopoulou P, Navarro P, Zanetti A, Lampugnani MG, Dejana E (1999) Histamine induces tyrosine phosphorylation of endothelial cell-to-cell adherens junctions. Arterioscler Thromb Vasc Biol 19:2286–2297. CrossRef Medline

Bartel DP (2009) MicroRNAs: target recognition and regulatory functions. Cell 136:215–233. CrossRef Medline

Chang JR, Mukerjee R, Bagashev A, Del Valle L, Chabrashvili T, Hawkins BJ, He JJ, Sawaya BE (2011) HIV-1 Tat protein promotes neuronal dysfunction through disruption of microRNAs. J Biol Chem 286:41125–41134. CrossRef Medline

Dejana E (2004) Endothelial cell-cell junctions: happy together. Nat Rev Mol Cell Biol 5:261–270. CrossRef Medline

Dejana E, Giampietro C (2012) Vascular endothelial-cadherin and vascular stability. Curr Opin Hematol 19:218–223. CrossRef Medline

Dejana E, Bazzoni G, Lampugnani MG (1999) Vascular endothelial (VE)-cadherin: only an intercellular glue? Exp Cell Res 252:13–19. CrossRef Medline

Dejana E, Orsenigo F, Lampugnani MG (2008) The role of adherens junctions and VE-cadherin in the control of vascular permeability. J Cell Sci 121:2115–2122. CrossRef Medline

Dewi BE, Takasaki T, Kurane I (2008) Peripheral blood mononuclear cells increase the permeability of dengue virus-infected endothelial cells in association with downregulation of vascular endothelial cadherin. J Gen Virol 89:642–652. CrossRef Medline

Eletto D, Russo G, Passiatore G, Del Valle L, Giordano A, Khalili K, Gualco E, Peruzzi F (2008) Inhibition of SNAP25 expression by HIV-1 Tat involves the activity of mir-128a. J Cell Physiol 216:764–770. CrossRef Medline

Fiore R, Khudayberdiev S, Christensen M, Siegel G, Flavell SW, Kim TK, Greenberg ME, Schratt G (2009) Mef2-mediated transcription of the miR379–410 cluster regulates activity-dependent dendritogenesis by fine-tuning Pumilio2 protein levels. EMBO J 28:697–710. CrossRef Medline

Frankel AD, Pabo CO (1988) Cellular uptake of the tat protein from human immunodeficiency virus. Cell 55:1189–1193. CrossRef Medline

Gandhi N, Saiyed Z, Thangavel S, Rodriguez J, Rao KV, Nair MP (2009) Differential effects of HIV type 1 clade B and clade C Tat protein on expression of proinflammatory and antiinflammatory cytokines by primary monocytes. AIDS Res Hum Retroviruses 25:691–699. CrossRef Medline

Gandhi N, Saiyed ZM, Napuri J, Samikkannu T, Reddy PV, Agudelo M, Khatavkar P, Saxena SK, Nair MP (2010) Interactive role of human immunodeficiency virus type 1 (HIV-1) clade-specific Tat protein and cocaine in blood-brain barrier dysfunction: implications for HIV-1-associated neurocognitive disorder. J Neurovirol 16:294–305. CrossRef Medline

Gavard J, Gutkind JS (2008) VE-cadherin and claudin-5: it takes two to tango. Nat Cell Biol 10:883–885. CrossRef Medline

Geretti AM (2006) HIV-1 subtypes: epidemiology and significance for HIV management. Curr Opin Infect Dis 19:1–7. CrossRef Medline

González-Scarano F, Martín-García J (2005) The neuropathogenesis of AIDS. Nat Rev Immunol 5:69–81. CrossRef Medline

Harris ES, Nelson WJ (2010) VE-cadherin: at the front, center, and sides of endothelial cell organization and function. Curr Opin Cell Biol 22:651–658. CrossRef Medline

Hazleton JE, Berman JW, Eugenin EA (2010) Novel mechanisms of central nervous system damage in HIV infection. HIV AIDS (Auckl) 2:39–49.

Hui L, Chen X, Bhatt D, Geiger NH, Rosenberger TA, Haughey NJ, Masino SA, Geiger JD (2012) Ketone bodies protection against HIV-1 Tat-induced neurotoxicity. J Neurochem 122:382–391. CrossRef Medline

John B, Sander C, Marks DS (2006) Prediction of human microRNA targets. Methods Mol Biol 342:101–113. Medline

Lampugnani MG, Resnati M, Raiteri M, Pigott R, Pisacane A, Houen G, Ruco LP, Dejana E (1992) A novel endothelial-specific membrane protein is a marker of cell-cell contacts. J Cell Biol 118:1511–1522. CrossRef Medline

Mahajan SD, Aalinkeel R, Sykes DE, Reynolds JL, Bindukumar B, Fernandez SF, Chawda R, Shanahan TC, Schwartz SA (2008) Tight junction regulation by morphine and HIV-1 tat modulates blood-brain barrier permeability. J Clin Immunol 28:528–541. CrossRef Medline

Miller F, Afonso PV, Gessain A, Ceccaldi PE (2012) Blood-brain barrier and retroviral infections. Virulence 3:222–229. CrossRef Medline

Mishra R, Chhatbar C, Singh SK (2012) HIV-1 Tat C-mediated regulation of tumor necrosis factor receptor-associated factor-3 by microRNA 32 in human microglia. J Neuroinflammation 9:131. CrossRef Medline

Nitta T, Hata M, Gotoh S, Seo Y, Sasaki H, Hashimoto N, Furuse M, Tsukita S (2003) Size-selective loosening of the blood-brain barrier in claudin-5-deficient mice. J Cell Biol 161:653–660. CrossRef Medline

Pacifici M, Delbue S, Ferrante P, Jeansonne D, Kadri F, Nelson S, Velasco-Gonzalez C, Zabaleta J, Peruzzi F (2013) Cerebrospinal fluid miRNA profile in HIV-encephalitis. J Cell Physiol 228:1070–1075. CrossRef Medline

Persidsky Y, Heilman D, Haorah J, Zelivyanskaya M, Persidsky R, Weber GA, Shimokawa H, Kaibuchi K, Ikezu T (2006) Rho-mediated regulation of tight junctions during monocyte migration across the blood-brain barrier in HIV-1 encephalitis (HIVE). Blood 107:4770–4780. CrossRef Medline

Poggi A, Carosio R, Fenoglio D, Brenci S, Murdaca G, Setti M, Indiveri F, Scabini S, Ferrero E, Zocchi MR (2004) Migration of V delta 1 and V delta 2 T cells in response to CXCR3 and CXCR4 ligands in healthy donors and HIV-1-infected patients: competition by HIV-1 Tat. Blood 103:2205–2213. CrossRef Medline

Pu H, Hayashi K, András IE, Eum SY, Hennig B, Toborek M (2007) Limited role of COX-2 in HIV Tat-induced alterations of tight junction protein expression and disruption of the blood-brain barrier. Brain Res 1184: 333–344. CrossRef Medline

Reese TS, Karnovsky MJ (1967) Fine structural localization of a blood-brain

barrier to exogenous peroxidase. J Cell Biol 34:207–217. CrossRef Medline

Samikkannu T, Saiyed ZM, Rao KV, Babu DK, Rodriguez JW, Papuashvili MN, Nair MP (2009) Differential regulation of indoleamine-2,3-dioxygenase (IDO) by HIV type 1 clade B and C Tat protein. AIDS Res Hum Retroviruses 25:329–335. CrossRef Medline

Santhakumar D, Forster T, Laqtom NN, Fragkoudis R, Dickinson P, Abreu-Goodger C, Manakov SA, Choudhury NR, Griffiths SJ, Vermeulen A, Enright AJ, Dutia B, Kohl A, Ghazal P, Buck AH (2010) Combined agonist-antagonist genome-wide functional screening identifies broadly active antiviral microRNAs. Proc Natl Acad Sci U S A 107:13830–13835. CrossRef Medline

Spindler KR, Hsu TH (2012) Viral disruption of the blood-brain barrier. Trends Microbiol 20:282–290. CrossRef Medline

Spudich SS, Ances BM (2011) Central nervous system complications of HIV infection. Top Antivir Med 19:48–57. Medline

Strazza M, Pirrone V, Wigdahl B, Nonnemacher MR (2011) Breaking down the barrier: the effects of HIV-1 on the blood-brain barrier. Brain Res 1399:96–115. CrossRef Medline

Taddei A, Giampietro C, Conti A, Orsenigo F, Breviario F, Pirazzoli V, Potente M, Daly C, Dimmeler S, Dejana E (2008) Endothelial adherens junctions control tight junctions by VE-cadherin-mediated upregulation of claudin-5. Nat Cell Biol 10:923–934. CrossRef Medline

Vincent PA, Xiao K, Buckley KM, Kowalczyk AP (2004) VE-cadherin: adhesion at arm's length. Am J Physiol Cell Physiol 286:C987–C997. Medline

Westendorp MO, Frank R, Ochsenbauer C, Stricker K, Dhein J, Walczak H, Debatin KM, Krammer PH (1995) Sensitization of T cells to CD95-mediated apoptosis by HIV-1 Tat and gp120. Nature 375:497–500. CrossRef Medline

Wong JK, Campbell GR, Spector SA (2010) Differential induction of interleukin-10 in monocytes by HIV-1 clade B and clade C Tat proteins. J Biol Chem 285:18319–18325. CrossRef Medline

Xiao H, Neuveut C, Tiffany HL, Benkirane M, Rich EA, Murphy PM, Jeang KT (2000) Selective CXCR4 antagonism by Tat: implications for in vivo expansion of coreceptor use by HIV-1. Proc Natl Acad Sci U S A 97:11466–11471. CrossRef Medline

Xu R, Feng X, Xie X, Zhang J, Wu D, Xu L (2012) HIV-1 Tat protein increases the permeability of brain endothelial cells by both inhibiting occludin expression and cleaving occludin via matrix metalloproteinase-9. Brain Res 1436:13–19. CrossRef Medline

Zhong Y, Smart EJ, Weksler B, Couraud PO, Hennig B, Toborek M (2008) Caveolin-1 regulates human immunodeficiency virus-1 Tat-induced alterations of tight junction protein expression via modulation of the Ras signaling. J Neurosci 28:7788–7796. CrossRef Medline

Zhu W, London NR, Gibson CC, Davis CT, Tong Z, Sorensen LK, Shi DS, Guo J, Smith MC, Grossmann AH, Thomas KR, Li DY (2012) Interleukin receptor activates a MYD88-ARNO-ARF6 cascade to disrupt vascular stability. Nature 492:252–255. CrossRef Medline

JOURNAL OF NEUROINFLAMMATION

RESEARCH Open Access

Regulatory role of TRIM21 in the type-I interferon pathway in Japanese encephalitis virus-infected human microglial cells

Gunjan Dhawan Manocha[1], Ritu Mishra[1], Nikhil Sharma[1], Kanhaiya Lal Kumawat[2], Anirban Basu[2] and Sunit K Singh[1*]

Abstract

Background: Japanese encephalitis virus (JEV) infection leads to Japanese encephalitis (JE) in humans. JEV is transmitted through mosquitoes and maintained in a zoonotic cycle. This cycle involves pigs as the major reservoir, water birds as carriers and mosquitoes as vectors. JEV invasion into the central nervous system (CNS) may occur via antipodal transport of virions or through the vascular endothelial cells. Microglial cells get activated in response to pathogenic insults. JEV infection induces the innate immune response and triggers the production of type I interferons. The signaling pathway of type I interferon production is regulated by a number of molecules. TRIM proteins are known to regulate the expression of interferons; however, the involvement of TRIM genes and their underlying mechanism during JEV infection are not known.

Methods: Human microglial cells (CHME3) were infected with JEV to understand the role of TRIM21 in JEV infection and its effect on type I interferon (IFN-β) production. Cells were infected in presence and absence of exogenous TRIM21 as well as after knocking down the TRIM21 mRNA. Levels of activated IRF3 expression were measured through Western blot analyses of anti-p-IRF3 antibody, and IFN-β production was measured by using IFN-β real-time PCR and luciferase activity analyses.

Results: JEV infection increased expression of TRIM21 in CHME3 cells. JEV induced an innate immune response by increasing production of IFN-β via IRF3 activation and phosphorylation. Overexpression of TRIM21 resulted in downregulation of p-IRF3 and IFN-β, while silencing led to increased production of p-IRF3 and IFN-β in JEV-infected CHME3 cells.

Conclusion: This report demonstrates TRIM21 as a negative regulator of interferon-β (IFN-β) production mediated by IRF-3 during JEV infection in human microglial cells.

Keywords: Japanese encephalitis virus, Viral encephalitis, Flavivirus, Antiviral mechanism, Immune evasion, TRIM proteins, TRIM21, Type I interferons, IRF-3, Vector borne infection

Background

Japanese encephalitis virus (JEV), a flavivirus with single-stranded RNA, is the leading cause of viral encephalitis in most of southeast Asian countries. JEV is transmitted through mosquitoes and maintained in a zoonotic cycle. This cycle involves pigs as the major reservoir/amplifying host, water birds as carriers and mosquitoes as vectors [1]. The estimated worldwide annual incidence of Japanese encephalitis (JE) is about 45,000 human cases and 10,000 deaths [2]. JE leads to long-term neurological damage and significant mortality among children. Approximately 25% of encephalitis patients die, while about 50% of the survivors develop permanent neurologic and/or psychiatric sequelae [1].

The flaviviruses are known to induce proinflammatory response in CNS after infection.

A key step toward induction of innate immunity against viral infections, including JEV, is the production of type I

* Correspondence: sunitsingh2000@gmail.com
[1]Laboratory of Neurovirology and Inflammation Biology, CSIR-Centre for Cellular and Molecular Biology (CCMB), New R&D Building-1st Floor, Uppal Road, Hyderabad 500007, India
Full list of author information is available at the end of the article

interferons. The presence of virus is sensed by pattern recognition receptors (PRRs) such as Toll-like receptors (TLRs) and RIG-I (retinoic acid-inducible gene 1)-like receptors (RLRs) [3,4]. The engagement of these (receptors) through pathogen molecular patterns can lead to the production of various cytokines and chemokines and other proinflammatory factors. The key regulators of the induction of type I IFNs during viral infections are RIG-I and MDA5 (melanoma differentiation-associated protein 5) [5-10]. These are known to interact with MAVS (mitochondrial antiviral signaling protein), which leads to downstream activation of various kinases such as TBK1/IKKε (TANK-binding kinase 1/I kappa B Kinase-ε), which in turn lead to phosphorylation and activation of various transcription factors to induce IFN-β and IFN-α [11-13]. The production of type I interferons is crucial for generating antiviral response against viruses. Production of interferons is mediated by various transcription factors such as interferon regulatory factors (IRF). Among the IRF family members, IRF-3 has been well documented to play a role in expression of type I interferons in response to viral infections. Phosphorylation of IRF-3 leads to activation, dimerization and nuclear translocation, ultimately leading to the transcription and production of IFN-β. IFN-β further initiates a cascade of signaling events mediated by IRF-7 and IRF-5 resulting in the production of IFN-γ and activation of various interferon-stimulated genes (ISGs) [8,14].

The TRIM family (tripartite-motif family) of proteins has been reported for their roles in regulating the innate immune response to viral infections [15]. TRIM proteins are structurally characterized by a RING domain, a B-box domain and a coiled-coil domain [16,17]. Functionally, most TRIMs are E3 ubiquitin ligases, where RING domains have ubiquitin ligase activity, while the b-Box domains have interacting motifs. TRIM proteins have been reported for their roles in cellular processes such as cell differentiation, transcriptional regulation, signaling cascades and apoptosis [15,18,19]. Many TRIM proteins play important roles in antiviral activities [20]. TRIM5 and TRIM22 are known to restrict HIV replication, while TRIM19 has been reported to restrict VSV and herpes simplex virus (HSV) replication [21-24]. TRIM21 has been known to play a crucial role in regulating type I interferon production, but its role during viral infections is not well understood [25,26]. TRIM21 interacts and ubiquitinates IRF-3, IRF-7 and IRF-8 [27]. Due to such interactions, TRIM21 has been implicated in regulating type I interferon signaling directly by modulating the upstream transcription factors. TRIM21 is part of the RoSSA ribonucleoprotein, which includes a single polypeptide and one of four small RNA molecules. TRIM21 has been reported to recognize and degrade viruses in the cytoplasm by binding to antibody-coated virions [28].

This is the first report showing the role of TRIM21 in modulating the type I interferon response upon JEV infection in human microglial cells. We have demonstrated that induction of TRIM21 during JEV infection is a compensatory mechanism to downregulate the type I interferon production mediated by IRF-3. TRIM21 overexpression leads to downregulation of JEV-mediated activation of IRF-3 and downstream IFN-β production, whereas silencing of TRIM21 results in facilitation of JEV-mediated activation of IRF-3 and upregulation of IFN-β production. We thereby report the inhibitory role of TRIM21 on IFN-β production during JEV infection in human microglial cells.

Materials and methods

Materials

The anti-p-IRF3 (Ser396) antibody (#4947S), anti-IRF3 antibody (#4302S), anti-IRF7 (#4920S) and anti-pIRF7 (#5184S) antibodies were purchased from Cell Signaling Technology (Danvers, MA, USA). Anti-β tubulin antibody (#Ab6046) was from Abcam (Cambridge, MA, USA), while anti-TRIM21 antibody (Ro52/SSA) (#sc-25351) was purchased from Santa Cruz Biotechnology (Santa Cruz, CA, USA). Dulbecco's Modified Eagle's Medium (DMEM) (#12100–046) was purchased from Gibco (Rockville, MD, USA). Transfection reagents, Lipofectamine 2000 (#1168-019) and GeneCellin (#GC1000) were from Invitrogen (Carlsbad, CA, USA) and BioCellChallenge, respectively. SiRNA against TRIM21 was purchased from Origene (Rockville, MD, USA) along with Negative control scrambled RNA (TRIM21 Trilencer-27 Human siRNA; #SR304594). IFN-β-luciferase promoter was a kind gift from Dr. Adolfo Garcia-Sastre (Mount Sinai School of Medicine, New York City, NY, USA) while JEV (genotype 1 strain # JaOAr) was gifted by Dr. Anirban Basu (NBRC, Manesar, India). Real-time PCR primers were obtained from Bioserve (Hyderabad, India) and IDT (Belgium, Europe).

Cell culture

Human microglial cell line (CHME3 cells), porcine stable kidney cell line (PS) (for plaque assay) and C6/36 cell line (for viral propagation) were cultured in DMEM (Invitrogen) containing 10% heat-inactivated fetal bovine serum, 100 U penicillin, 100 g/ml streptomycin (#15140122; Invitrogen, Carlsbad, CA, USA) and L-glutamine. All cells were grown in humidified atmosphere containing 5% CO_2 and 95% air at 37°C (CHME3 and PS cells) and 28°C (C6/36 cells).

JEV propagation, plaque assay and infection

JEV (genotype 1, JaOAr) was a kind gift from Dr. Anirban Basu, NBRC, India. JEV was further propagated in C6/36

cells. Briefly, C6/36 cells were infected with JEV (MOI 2) in 75 cm^2 (T-75) cell culture flasks and incubated for 7 days. Post infection, supernatant was collected and precipitated using a PEG viral precipitation kit (#ab102538; Abcam, Cambridge, MA, USA). Plaque-forming units (PFU) of the propagated virus were determined by plaque assay by using porcine stable kidney cells (PS). Cells were seeded at a density of 1.6×10^5 cells in six-well plates and infected with JEV at different dilutions ranging from 10^{-3} – 10^{-10} for 2 h. Post infection, cells were washed with PBS, and 2% low melting agarose overlay [containing 2X-DMEM, 5% FBS and 1% antibiotic (penicillin-streptomycin)] was added to each well. Plates were then incubated at 37°C, 5% CO_2, for 96 h. Viral plaques were fixed with 10% HCHO and stained with crystal violet in order to count the number of plaques and determine the PFU for JEV. Further infection experiments in this study were performed using JEV at a multiplicity of infection (MOI) of 5 for 24 h, unless otherwise noted. For infection experiments, CHME3 cells were infected with JEV at an MOI of 5 in incomplete DMEM alone for 3 h. Incomplete media were replaced by complete growth media (DMEM with 10% FBS and antibiotics) 3 h later. Cells were harvested at 24 h post infection for RNA and/or protein isolation.

TRIM21 overexpression and knockdown

TRIM21 was cloned into the pcDNA3.1 vector. The product was sequenced for confirmation and transformed into DH5α competent cells. The plasmid was then isolated using Qiagen maxi-prep kit (#12163; Qiagen, Hilden, Germany) and observed on a 0.8% agarose gel for purity. A truncated form of TRIM21 without the N-terminal RING domain was also cloned into the pcDNA3.1 vector, to be known as TRIM21 (ΔRING) in this study. TRIM21 protein is comprised of a RING domain from the 16th – 54th amino acid. Therefore, the TRIM21 (ΔRING) primers were designed in such a way that the reverse primer was similar to the wild-type TRIM21 clone, while the forward primer was designed such as to start the polymerase reaction from the 163rd nucleotide so that the RING domain from the wild-type TRIM21 sequence was completely removed. The PCR product was checked on an agarose gel (Figure 1A). The PCR product was further eluted out of agarose gel and digested using EcoR1 and HINDIII enzymes. Along with this insert, the pcDNA3.1 vector was also digested using the same enzymes. Following digestion, the vector and insert were ligated using T4 ligase at 15°C overnight. The ligated product was transformed into *E. coli* DH5α competent cells and spread on an LA agar plate with ampicillin and incubated at 37°C for 15–16 h. The resultant colonies were checked with PCR using TRIM21 (ΔRING) primers, and the positive colonies were further inoculated in LB media to isolate the plasmid using the Qiagen miniprep kit (#27104, Qiagen, Hilden, Germany) according to manufacturer's protocol. The resultant plasmid was validated by sequencing and used for transfection studies. To validate the expression of truncated TRIM21, CHME3 cells were transfected with TRIM21 (WT) and TRIM21 (ΔRING) for 48 h. Lysates were resolved on SDS-PAGE and probed with for anti-TRIM21 antibody by Western blot. For overexpression, 1 day prior to transfection, CHME3 cells were seeded in 25 cm^2 cell culture flasks at 70% confluency. Cells were transfected with 4 μg of either TRIM21 or TRIM21 (ΔRING) plasmid per 600,000 cells using GeneCellin transfection reagent in 4 ml transfection media (DMEM with 10% FBS). Cells were replenished with complete growth media (DMEM + 10% FBS + antibiotics) after 8 h of transfection and incubated for 48 h. In cases of infection experiments, 24 h post transfection, cells were infected with JEV at MOI 5 and lysed 24 h post infection. In case of silencing of TRIM21, siRNA against TRIM21 was transfected to CHME3 cells in six-well plates (1.5×10^5 cells per well) using Lipofectamine 2000 transfection reagent. Cells were either non-transfected (control), transfected with scrambled RNA provided in the siRNA kit (negative control) or transfected with siRNA duplex for 48 h. Cells were infected 24 h post transfection in the experiments wherever required.

Western blotting

Cells were transfected with TRIM21 plasmid for overexpression studies and siRNA for silencing studies as described above. After 48 h of transfection, cells were lysed using RIPA (150 mM NaCl, 50 mM Tris–HCl, pH 7.5, 1% NP-40, 0.5% sodium deoxycholate, 0.1% SDS) buffer containing 1 μM PMSF and 1X protease inhibitor cocktail, ProteCEASE-50 (#427P; G-Biosciences, St. Louis, MO, USA). Protein was quantified using Bradford assay [29]. Lysates were resolved on SDS-PAGE and Western blotted using the desired antibodies against p-IRF3 (1:3,000 dilution), IRF3 (1:3,000), TRIM21 (1:5,000), p-IRF7 (1:3,000) and IRF7 (1:3,000). Optical densities for p-IRF3, p-IRF7 and TRIM21 from visualized Western blots were normalized to their respective loading controls (IRF3/IRF7/β-tubulin) and averaged from three independent experiments.

Real-time PCR

For RNA isolation, cells were harvested and total RNA isolated using Qiagen RNeasy kit (#74106; Qiagen, Hilden, Germany). Synthesis of cDNA was performed using Superscript II reverse transcriptase system (#11904-018; Invitrogen, Carlsbad, CA, USA) according to manufacturer's protocol using 2,000 ng RNA. Thermal cycles of cDNA synthesis using random hexamers were as follows: 65°C (5 min); 25°C (10 min); 42°C (50 min); 70°C (10 min); followed by treatment with RNase H for 20 min at 37°C. For amplification, 100 ng cDNA was used as a

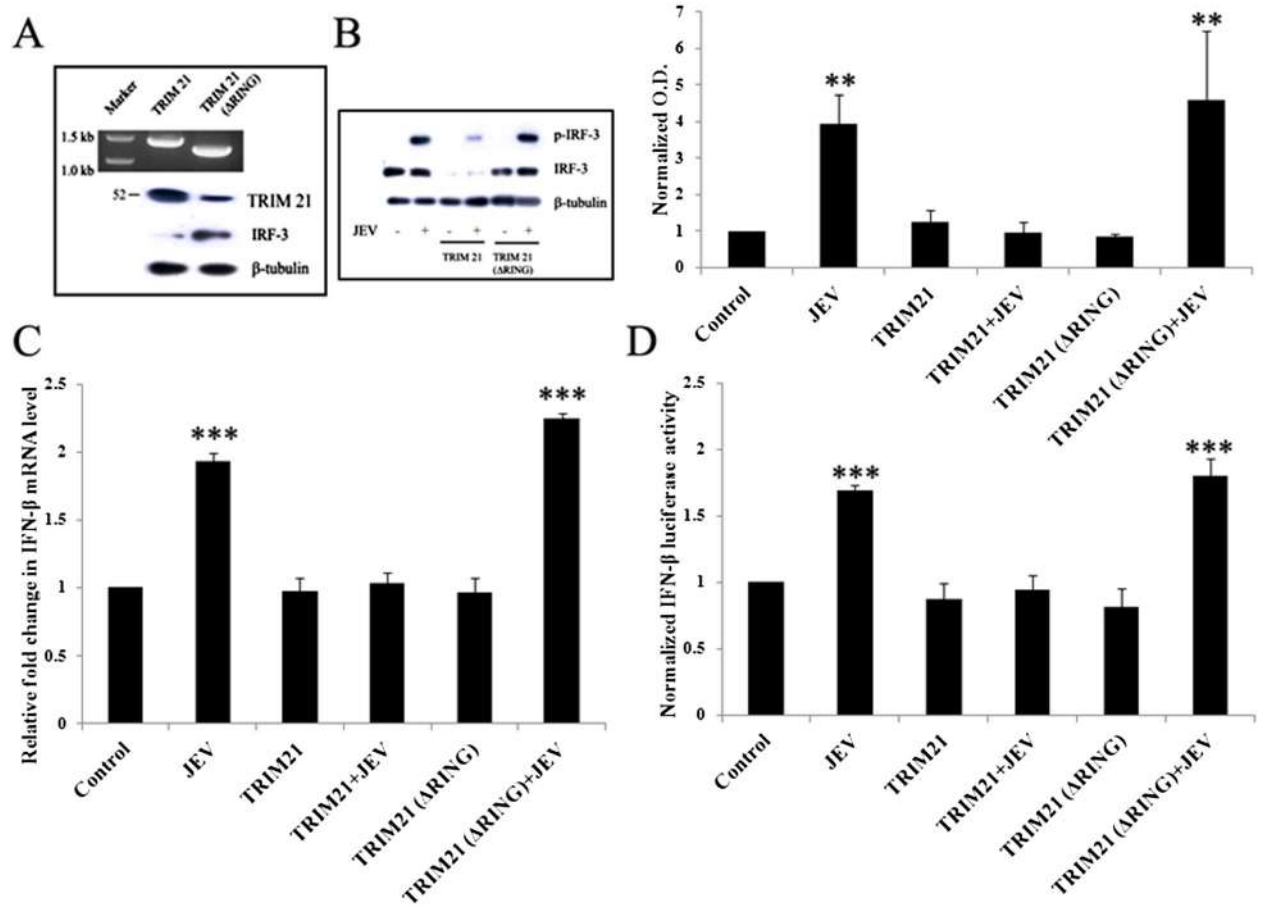

Figure 1 TRIM21 attenuates the JEV mediated upregulation of the p-IRF3 level and IFN-β level in human microglial cells. (A) PCR amplification of TRIM21 and TRIM21 (ΔRING) primers was carried out and the product run on 1% agarose gel (*upper panel*). Expression of wild-type TRIM21 as well as the TRIM21 (ΔRING) domain was confirmed by Western blotting (*lower panel*). **(B)** CHME3 cells were transfected with 4 μg of TRIM21 plasmid or TRIM21 (ΔRING) for 48 h. Cell lysates were resolved on *SDS*-PAGE and probed with anti-TRIM21, anti-IRF-3 and anti-β-tubulin antibodies by Western blotting. Representative image is shown. **(C)** Cells transfected with TRIM21 or TRIM21 (ΔRING) were infected with JEV, and total RNA was isolated post 48 h of transfection. Real-time PCR for *IFN-β1* was performed, and an average of three independent sets of experiments is plotted and shown. **(D)** Luciferase assay for IFN-β for cells transfected with TRIM21 or TRIM21 (ΔRING) and infected with JEV along with respective controls was performed. Luciferase activity normalized against β-gal activity was averaged and plotted (*p <0.05, **p < 0.01, ***p < 0.001 from control).

template for performing RT-PCR using SYBR Green Supermix (#4367659; Applied Biosystems, Warrington, UK). Sequences of all the primers used for various genes in this study are mentioned in Table 1.

IFN-β luciferase assay

CHME3 cells were seeded at a density of 65,000 cells per well in 12-well Plates 1 day prior to transfection. Cells were transfected with IFN-β-Luc reporter plasmid (1 μg/ml) and β-gal (350 ng/ml) in 1 ml of transfection media (DMEM + 10% FBS). In case of TRIM21 overexpression, 1 μg/ml TRIM21 plasmid was co-transfected, while in case of knockdown, 10nM siRNA for TRIM21 was co-transfected. In conditions where infection was required, cells were infected with JEV (MOI 5) 24 h post transfection. After 48 h of transfection (24 h after

Table 1 List of primers

Gene name	Primer sequence (5′-3′)
TRIM21	Fwd: 5′ AGAGAGACTTCACCTGTTCTGT 3′
	Rev: 5′ TCAGTTCCCCTAATGCCACCT 3′
TRIM21 (ΔRING)	Fwd: 5′ TACGAATTCCGGCAGCGCTTTCTGCTC 3′
	Rev: 5′ GCCAAGCTTATAGTCAGTGGATCCTTG 3′
IFN-β1	Fwd: 5′ GCTCTCCTGTTGTGCTTCTCCAC 3′
	Rev: 5′ CAATAGTCTCATTCCAGCCAGTGC 3′
β-Actin	Fwd: 5′ GTCTGCCTTGGTAGTGGATAATG 3′
	Rev: 5′ TCGAGGACGCCCTATCATGG 3′

infection), cells were harvested and luciferase assay performed using the Luciferase assay kit (#E4030; Promega, Madison, WI, USA) according to the manufacturer's protocol. Cells were lysed in 150 μl 1X lysis buffer and centrifuged at 12,000 g for 3 min, and the supernatant was used for luminescence measurement using the Luciferase assay reagent. Normalization was done by performing a β-galactosidase assay using the β-galactosidase kit (#E2000; Promega, Madison, WI, USA). For this assay, 50 μl of the lysate supernatant was incubated with 50 μl 2X assay buffer at 37°C for 30 min, and the resulting yellow color was read at 420 nm. β-gal activity (in milliunits) in each of the lysates was obtained using a standard curve, and IFN-β luciferase activity was normalized (against β-gal activity), averaged and plotted for three independent sets of experiments.

Statistical analysis

Data are presented as mean ± standard error. Statistical significance was calculated by using one-way ANOVA and/or Student's *t*-test. The Tukey-Kramer multiple comparisons post hoc test was used to determine *P*-values.

Results

JEV induces IFN-β production in a time-dependent manner in human microglial cells

In order to verify the innate immune response being generated during JEV infection, we studied the level of IFN-β mRNA as well as IFN-β luciferase activity in microglial cells. Human microglial cells (CHME3) were infected with JEV at an MOI of 5 and harvested at various time intervals of 6, 12, 24 and 36 h. Infected cells were lysed using the reporter lysis buffer for the IFN-β-luciferase assay. IFN-β luciferase activity increased with JEV infection in a time-dependent manner until 24 h (Figure 2A). Since the maximal increase in IFN-β levels was observed at 24 h, all further experiments were performed at the 24-h time point. CHME3 cells were infected with JEV (MOI 5) for 24 h and harvested for RNA isolation. As seen in Figure 2B, IFN-β mRNA levels were significantly increased with JEV infection over the control (Figure 2B). These data confirm the activation of an immune response in terms of IFN-β production following JEV infection in CHME3 cells.

JEV induces phosphorylation of interferon regulatory factor-3

In most of the viral infections, the production of type I interferon is a key host immune response. This is mediated by various interferon regulatory factors such as IRF-3 (interferon regulatory factor-3) and IRF-7 (interferon regulatory factor-7). JEV-infected CHME3 cells showed significantly higher levels of active, phosphorylated IRF-3 as compared to controls (Figure 3A). An increase in p-IRF3 levels as seen by Western blotting corresponds with the production of IFN-β (Figure 2), observed at 24 h of JEV infection. Alternatively, IRF-7 phosphorylation was not affected in CHME3 cells infected with JEV at MOI 5 for 24 h (Figure 3B).

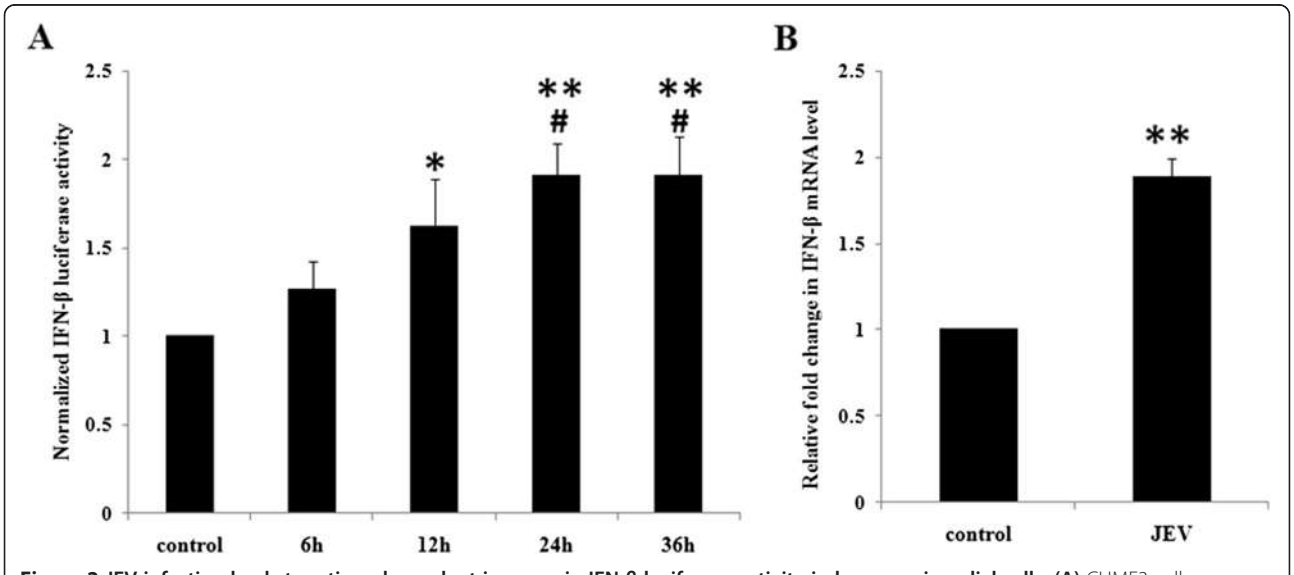

Figure 2 JEV infection leads to a time-dependent increase in IFN-β luciferase activity in human microglial cells. (A) CHME3 cells were transfected with IFN-β-luciferase promoter plasmid and β-gal promoter plasmid and infected with JEV at MOI 5 for 6, 12, 24 and 36 h. Luciferase activity was measured, normalized and averaged for three independent experiments. **(B)** CHME3 cells were infected with JEV at MOI 5 for 24 h and total RNA isolated and quantified by real-time PCR for *IFN-β1* levels. Fold change of the *IFN-β1* mRNA level for three independent experiments was averaged and plotted (*$p < 0.05$, **$p < 0.01$, ***$p < 0.001$ from control, $^{\#}p$ from 6 h, $^{\$}p$ from 12 h).

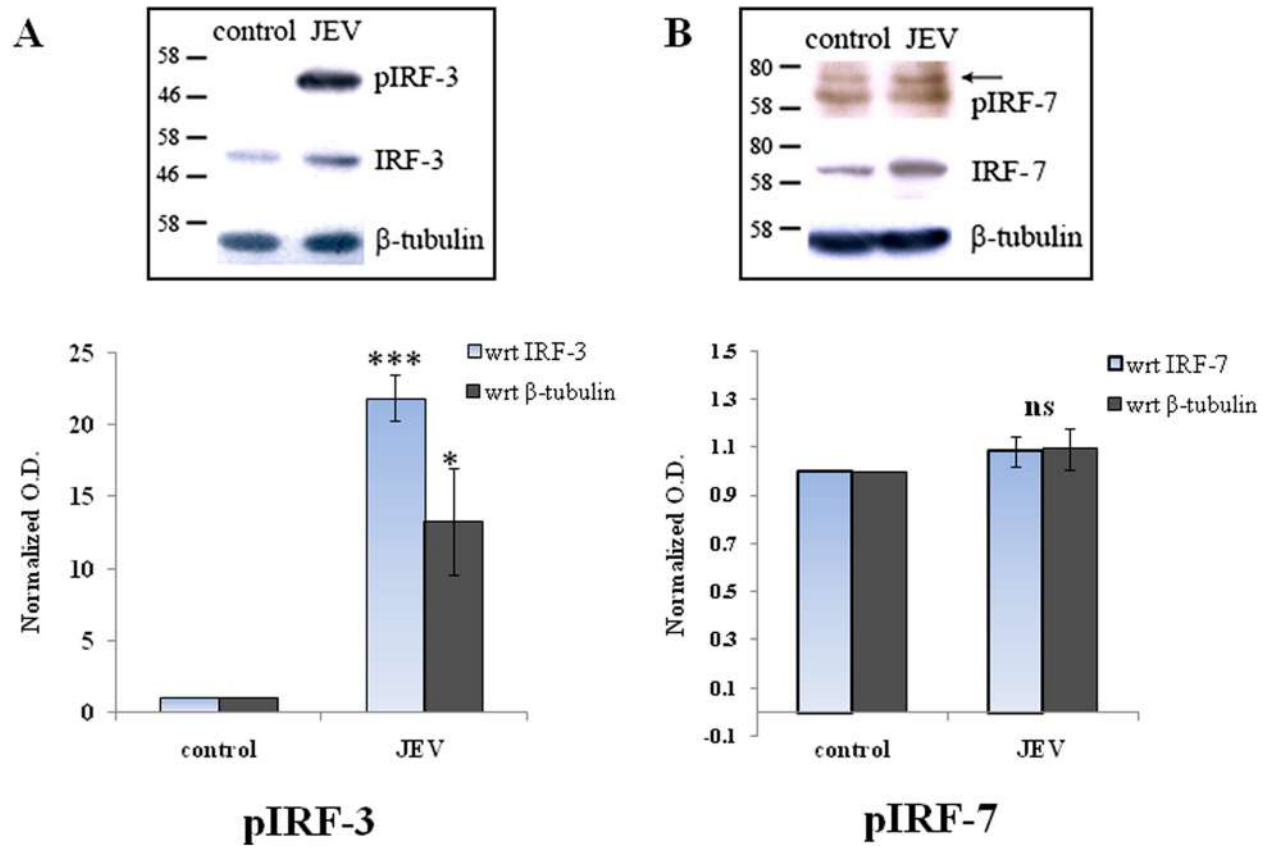

Figure 3 JEV induces phosphorylated IRF-3 levels in human microglial cells. (A) CHME3 cells were either un-infected or infected with JEV at MOI 5 for 24 h. Cell lysates were resolved on SDS-PAGE and probed with anti-p-IRF3 antibody, anti-p-IRF7, anti-IRF3 and anti-IRF7 antibodies, and anti-β-tubulin antibody (loading control) by Western blotting. Representatives of three independent experiments are shown. **(B)** Densitometry analyses of Western blot experiments were performed with normalizing p-IRF-3 and p-IRF-7 against their respective controls IRF-3 and IRF-7 as well as against β-tubulin (***p <0.001, *p < 0.05 from control).

JEV infection induces the expression of TRIM21 in human microglial cells in a time-dependent manner

TRIM21, an autoantigen, is known to interact with IRF-3, IRF-7 and IRF-8. Because of these interactions, it is a key regulator of the type I interferon immune response. TRIM21 is an E3 ubiquitin ligase that can interact with and ubiquitinate its target molecules. Since JEV induces p-IRF3 and IFN-β expression in human microglial cells (CHME3), we tried to understand the role of TRIM proteins, specifically TRIM21, in regulation of the type I interferon pathway. In order to identify the involvement of TRIM21 in JEV-infected CHME3 cells, we first determined the effect of JEV on the TRIM21 level in the cells. CHME3 cells were infected with JEV (MOI 5) and harvested at various time points. TRIM21 codes for 52 KDa RoSSA protein and Western blotting against the antibody for this protein (from hereon called TRIM21 protein) showed a time-dependent increase in TRIM21 levels for up to 36 h (Figure 4A). CHME3 cells infected with JEV at MOI 5 for 24 h showed increased mRNA levels for the TRIM21 gene (Figure 4B). Additionally, a time-course experiment for JEV infection was performed in HeLa cells to observe the expression of IFN-β as well as TRIM21. Although IFN-β levels increased upon JEV infection after 12 h, there was no change in TRIM21 levels in HeLa cells following JEV infection at any given time point (Additional file 1: Figure S1A & B). This suggested that the role of TRIM21 during JEV infection is specific to human microglial cells.

TRIM21 overexpression attenuates JEV-mediated upregulation of p-IRF3

Since TRIM21 interacts with IRF-3 directly, it has an important regulatory role in the immune response. We hypothesized that the upregulation of TRIM21 in JEV-infected cells could be a mechanism toward counteracting the production of type I interferons and/or an antiviral response towards the virus infection. The exogenous TRIM21 may further enhance this counteraction and may attenuate the effects in JEV-infected CHME3 cells in terms of

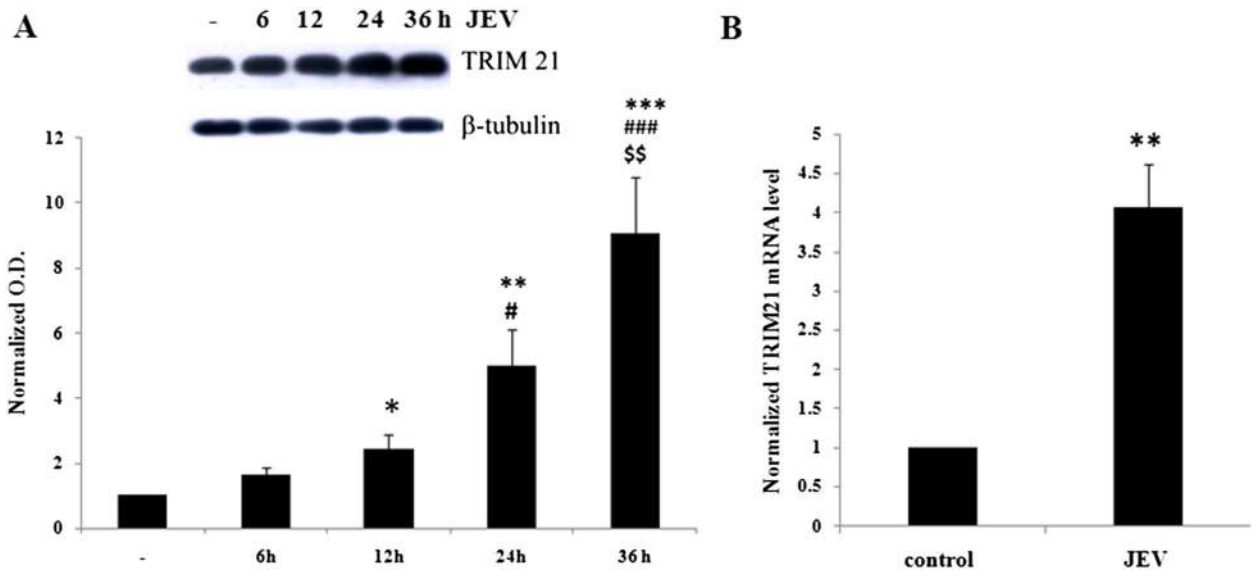

Figure 4 JEV induces TRIM21 protein levels in human microglial cells in a time-dependent manner. (A) CHME3 cells were either un-infected or infected with JEV at MOI 5 for 6, 12, 24 and 36 h. Cell lysates were resolved on SDS-PAGE and probed with anti-TRIM21 antibody and anti-β-tubulin antibody (loading control) by Western blotting. A representation of three independent experiments is shown along with densitometry analysis with normalization of TRIM21 against β-tubulin, averaging and plotting. **(B)** CHME3 cells were infected with JEV for 24 h (MOI 5). Total RNA was isolated from harvested cells. cDNA prepared by reverse transcription of control and infected samples was used as a template for qPCR against primers for *TRIM21* gene. Average fold change in the *TRIM21* mRNA level from three independent experiments is plotted and shown (*$p < 0.05$, **$p < 0.01$, ***$p < 0.001$ from control, $^{\#}p$ from 6 h, $^{\$}$p from 12 h).

IRF3 phosphorylation. Therefore, TRIM21 was overexpressed in CHME3 cells via plasmid transfection in order to observe the effect of TRIM21 on the IRF-3 level and JEV-mediated IRF-3 phosphorylation. The presence of exogenous TRIM21 and TRIM 21 (ΔRING) in CHME3 cells was observed through Western blotting studies. As shown in Figure 1A, TRIM21-transfected CHME3 cells showed TRIM21 antibody reactivity by Western blotting at 52 KDa, while cells transfected with TRIM 21 (ΔRING) showed a band slightly lower than the 52 KDa mark. Cells transfected with TRIM21 were infected by JEV after 24 h of transfection, and lysates were probed for phosphorylated IRF3 levels by Western blotting. As expected, JEV infection increased p-IRF3 levels in CHME3 cells as compared to control (GFP vector-transfected controls). However, overexpression of TRIM21 prior to infection resulted in a reduction of p-IRF3 levels post infection compared to the CHME3 cells only infected with JEV without TRIM21 transfection (Figure 1B). This suggests that TRIM21 could result in attenuation of JEV-mediated IRF-3 activation. Therefore, TRIM21 had an inhibitory effect on IRF3 activation. The total IRF-3 level was unaltered in the CHME3 cells infected with JEV, but TRIM21 overexpression reduced the level of total IRF3. This suggests that TRIM21 directly inhibits unphosphorylated IRF-3 in the presence or absence of JEV infection. This was further validated by using TRIM21 (ΔRING) plasmid in transfection studies. TRIM21 lacking the RING domain had no effect on the IRF3 level (Figure 1A,B). As a result, p-IRF3 levels were also not attenuated in TRIM21 (ΔRING)-transfected CHME3 cells following JEV infection (Figure 1B).

TRIM21 overexpression represses JEV-mediated elevation in IFN-β levels

We observed an increased production of IFN-β in JEV-infected CHME3 cells (Figure 2). Since TRIM21 transfection attenuates the activation of IRF3, it can be expected that TRIM21 leads to downstream inhibitory effects as well. Hence, in order to understand the role of TRIM21 on IFN-β production, we checked the levels of IFN-β mRNA as well as IFN-β luciferase activity in TRIM21-overexpressed CHME3 cells. Human IFN-β is encoded by the *IFN-β1* gene. CHME3 cells were transfected with TRIM21 plasmid and infected with JEV 24 h post transfection. The CHME3 cells were harvested and RNA isolated for real-time quantification of the *IFN-β1* mRNA level using the primers mentioned in Table 1, and fold change in the mRNA level was determined by normalizing the *IFN-β1* C_t values against those of *β-actin*. As observed in Figure 2B, we found an increased expression of *IFN-β1* at mRNA levels in JEV-infected CHME3 cells as compared to vector controls (Figure 1C). However, we observed the reduction in *IFN-β1* levels in JEV-infected TRIM21-transfected CHME3 cells in accordance with IRF-3 activation compared to controls. CHME3 cells transfected with truncated TRIM21 lacking the RING

domain showed no reduction in *IFN-β1* mRNA levels. A similar trend was observed with IFN-β luciferase activity. Cells were transfected with IFN-β-luciferase promoter and β-gal with or without TRIM21 plasmid followed by JEV infection. Luciferase activity was measured 48 h post transfection. JEV-infected cells showed significantly higher luciferase activity of IFN-β-luciferase promoter; however, transfection of TRIM21 before JEV infection attenuated JEV-mediated luciferase activity (Figure 1D). This observation suggests that TRIM21 has an inhibitory role in interferon-β production after JEV infection.

TRIM21 silencing facilitates JEV-mediated upregulation of the p-IRF3 level in CHME3 cells

To further confirm the inhibitory role of TRIM21 on IFN-β production, siRNA against TRIM21 was used to knock down the expression of TRIM21 in CHME3 cells. Silencing of TRIM21 was performed by using commercially available siRNA duplexes against TRIM21 that resulted in >70% knockdown of TRIM21 as shown in Figure 5A. Since JEV infection stimulated IRF3 activation and phosphorylation, this phenomenon was checked following TRIM21 silencing. JEV-infected CHME3 cells showed increased phosphorylation of IRF3 as compared to controls; however, silencing of TRIM21 prior to infection further enhanced the phosphorylation and activation of IRF3 (Figure 5B). This further confirmed the inhibitory role of dysregulated endogenous TRIM21 during JEV infection in human microglial cells.

TRIM21 silencing upregulates the JEV-mediated increase in IFN-β level

Further downstream from IRF3 activation, the expression level of IFN-β was checked in order to confirm the

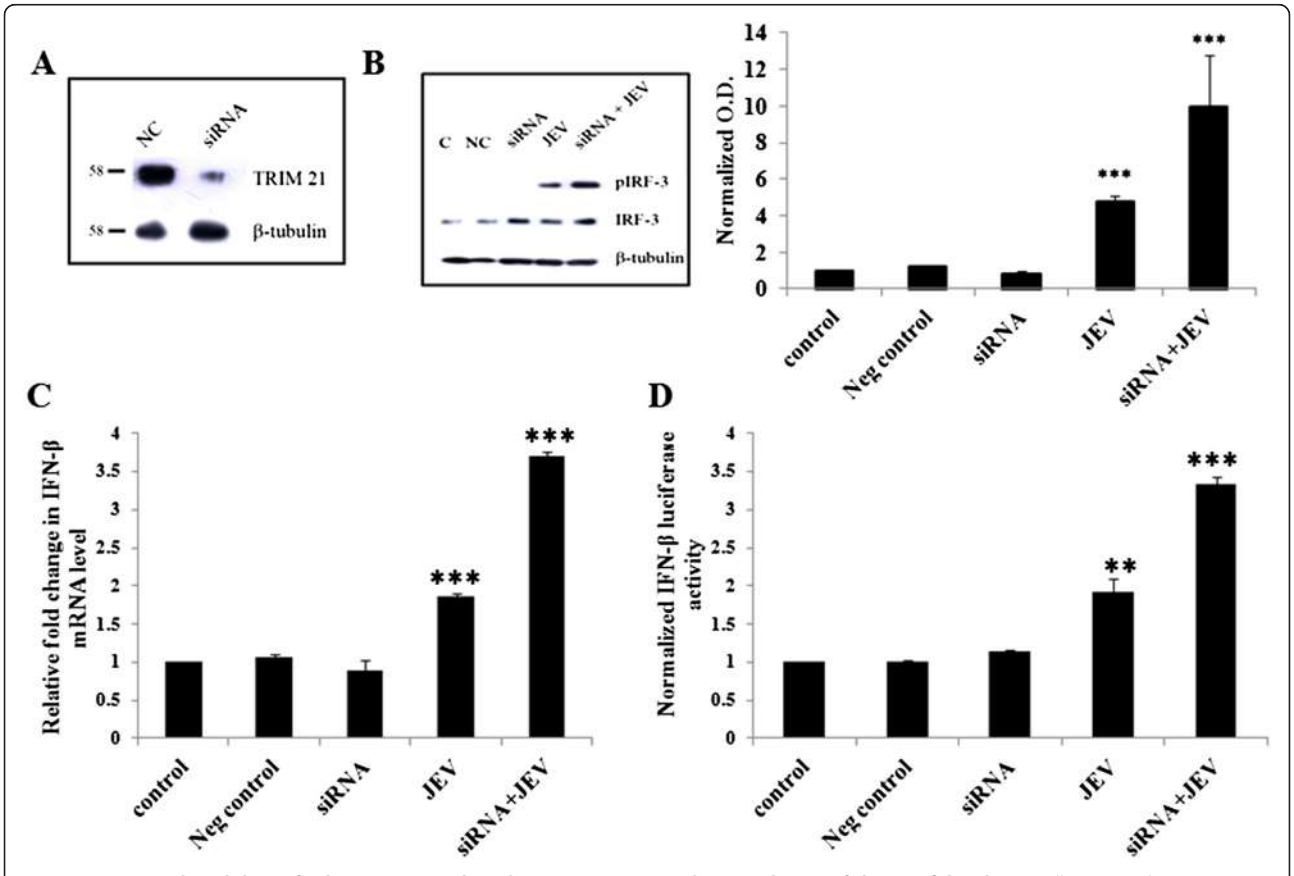

Figure 5 TRIM21 knockdown facilitates JEV-mediated IRF3 activation and upregulation of the IFN-β level. (A) Cells were either transfected with negative control RNA (*NC*) or transfected with 10nM siRNA against TRIM21 for 48 h. Cell lysates were resolved on SDS-PAGE and probed with anti-TRIM21 antibody and anti-β-tubulin antibody by Western blotting. A representative image is shown. **(B)** Cells were either non-transfected (C), transfected with negative control RNA (NC) or with TRIM21 siRNA for 24 h followed by JEV infection for 24 h. Cell lysates were resolved on SDS-PAGE and probed with anti-p-IRF3 antibody, anti-IRF3 and anti-β-tubulin antibodies (loading control) by Western blotting. A representative of three independent experiments is shown. Densitometry analyses of Western blot experiments were performed with normalizing p-IRF-3 and p-IRF-3 against β-tubulin. **(C)** Real-time PCR for *IFN-β1* for siRNA-transfected and JEV-infected cells along with the respective controls was performed and averaged for three independent sets of experiments. **(D)** Luciferase assay for IFN-β for cells transfected with siRNA against TRIM21 and infected with JEV along with respective controls was performed. Luciferase activity normalized against β-gal activity was averaged and plotted (**$p < 0.01$, ***$p < 0.001$ from control).

role of TRIM21 in modulating the expression of the interferon in case of JEV infection. Again, corresponding to the IRF3 activation, JEV-infection resulted in an additional increase in the IFN-β mRNA level as well as IFN-β-luciferase activity in CHME3 cells, where TRIM21 was silenced prior to the JEV infection (Figure 5C,D).

Discussion

This study reports that JEV infection induces the expression of TRIM21 in human microglial cells. Exogenous overexpression of TRIM21 attenuates JEV-mediated activation and phosphorylation of IRF3 as well as expression of IFN-β levels. In addition, TRIM21 silencing leads to facilitation of JEV-mediated IRF3 phosphorylation and downstream induction of IFN-β.

We demonstrated that JEV induces IRF3 activation at 24 h of JEV infection. However, levels of phosphorylated IRF7 are not significantly different in the infected cells as compared to control after 24 h. IRF7 has been reported to become activated only during the early phases of JEV infection, and the levels of p-IRF7 are not elevated during late phases of JEV infection [30]. Therefore, our study was focused on understanding the role of TRIM protein during JEV infection in the type I interferon pathway in terms of IRF3 activation as well as its effect on the expression of IFN-β. The production of IFN-β by JEV is known to occur through the RIG-1-mediated pathway [3]. However, the role of TRIM proteins in modulating the immune response in JEV infection had not yet been reported.

TRIM proteins are known to act as antiviral molecules because of their specific actions against specific viruses, as well as regulators of immune signaling pathway [15,25,31,32]. TRIM79α is reported to restrict viral replication of the tick-borne encephalitis virus (TBEV), but not other flaviviruses, such as West Nile virus [33]. TRIM56 has been reported to restrict bovine viral diarrhea virus replication *in vitro* [34]. The antiviral activity of TRIM21 has been reported to be through the antibody-mediated pathway [28,35]. It targets the virus toward proteasomal degradation by ubiquitination. Vaysburd *et al.* [28] showed that sensing of antibody-coated pathogens through TRIM21 increased in the case of nonenveloped DNA viruses, RNA viruses and intracellular bacterial infections [28,35]. While TRIM21 acts as an Fc receptor in sensing the antibody-coated viruses, the modulation of the immune signaling pathway by TRIM21 is dependent on the targeting of interferon regulatory factors via ubiquitination. We observed that JEV increases the expression of TRIM21 in CHME3 cells as a negative regulator of the type I interferon-mediated pathway. Two schools of thoughts exist regarding the action of TRIM21 in modulating the interferon pathway [25-27,36-38]. One suggests that TRIM21 promotes degradation of IRF-3 and IRF-7, thereby limiting type I interferon production. Our study supports the same findings as we observed the degradation of IRF-3 by TRIM21 in CHME3 cells; hence, the availability of less phosphorylated forms of IRF-3 ultimately leads to reduced expression of IFN-β [26,37]. Since there was no change in IRF3 levels and subsequent IFN-β levels upon TRIM21 (ΔRING) transfection, it suggested that the E3 ligase activity of TRIM21 may be responsible for the regulation of IRF3 expression. Our finding supports the those of Higgs *et al.* [26] in which they showed that both the RING domain and the SPRY domain are equally required to regulate the expression of IRF3 by the interaction and proteasomal degradation of IRF3 [26]. Hence, the absence of any one of the domains is sufficient to validate the role of TRIM21 in IRF3 and IFN-β regulation during JEV infection. The other school of thought supports the stabilization of IRF3 expression through a TRIM21-mediated pathway. This has been reported in the case of Sendai virus infection, where TRIM21 acts as a positive regulator of the IRF3 pathway during viral infection [27]. This functional variability could be attributed to being dependent on the type of viral infection, the duration of infection and the upstream signaling pathway. Apart from RNA virus recognition, TRIM21 is also able to modulate DNA virus infections. TRIM21 has been shown to interact with DDX41, a cytosolic DNA sensor that triggers type I IFN responses [39]. TRIM21 causes ubiquitination of DDX41, leading to a lesser production of IFN-β. A number of other TRIM proteins are also involved in modulating the inflammatory signaling pathways. TRIM30 (TRIM79α) is reported to be involved in lysosomal degradation of TAK1 binding protein 2 (TAB2) and TAK1 binding protein 3 (TAB3) downstream of the TLR4 pathway, leading to the inhibition of NF-κB induction during LPS stimulation [40]. Like TRIM21, TRIM27 is also known to target IKKs, thereby negatively regulating PRR pathways [41]. TRIM5α is also known to negatively regulate NF-κB and mitogen-activated protein kinase (MAPK) signaling pathways by targeting TGF-β-activated kinase 1 (TAK1), and these activities are known to be uncoupled from the retroviral capsid recognition [42,43]. TAK1 has also been reported to be targeted by TRIM8 [44]. TRIM5α has also been reported to positively regulate NF-κB signaling, AP-1 activation and expression of proinflammatory cytokines [42]. TRIM23 acts as a cofactor in the regulation of NF-κB activation in human cytomegalovirus infection [45]. Therefore, the modulation of immune responses by TRIM proteins can be highly specific based on the type of pathogens and their derivatives.

The increased expression of TRIM21 during JEV infection and its inhibitory role act as a feedback mechanism to attenuate the immune response (Figure 6). This is supported by the observation that the activation of IRF3 in JEV infection is further enhanced by knockdown of

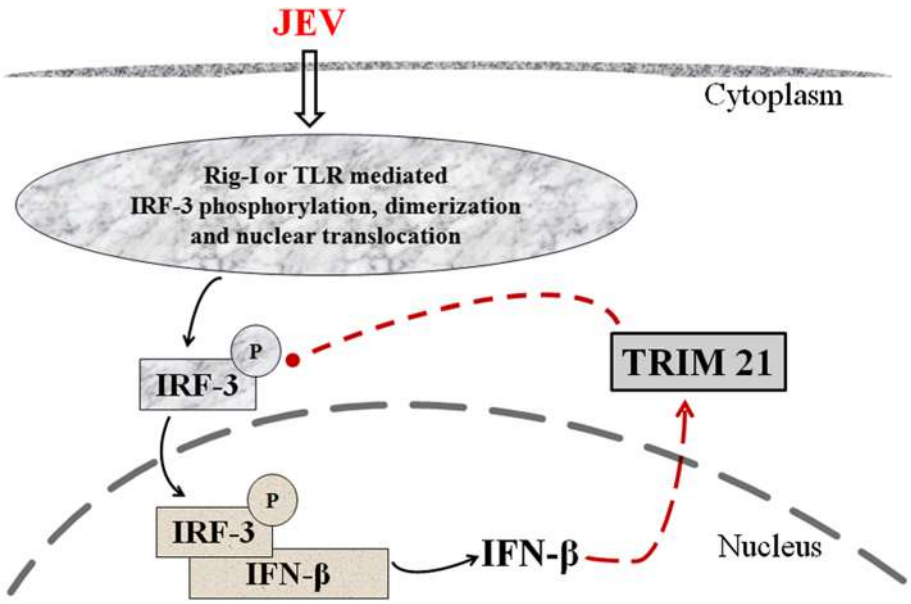

Figure 6 Model showing a plausible role of TRIM21 as a negative regulator of IRF3 activation and IFN-β production following JEV infection in human microglial cells. JEV infection causes activation of the RIG-1 receptor, initiating a downstream signaling mechanism leading to the activation of IRF-3. Phosphorylated IRF-3 dimerizes and translocates into the nucleus, where it leads to the transcription and production of IFN-β. JEV infection also induces the TRIM21 protein, which negatively regulates IRF-3 phosphorylation, leading to reduced IFN-β production. The upregulation of TRIM21 is proposed to be a feedback mechanism to inhibit the innate immune response in JEV infection.

TRIM21 in CHME3 cells prior to infection. Consequently, the IFN-β level was also increased in JEV-infected TRIM21 knocked-down cells. The expression of TRIM21 has also been reported to be induced by IFN-α and IFN-β via the IRF-mediated pathway [46]. Other TRIM proteins, such as TRIM5α and TRIM19, can also be altered by type I IFNs [47-51]. Two independent studies have reported the expression of many TRIM proteins following type I interferon stimulation in mouse macrophages, dendritic cells, primary human-monocyte-derived macrophages and human primary lymphocytes [47,48]. Zhao *et al.* [52] reported that TRIM 38 acts as a negative feedback regulator of NF-κB signaling in TLR agonist-treated macrophages [52]. This evidence along with our observations suggests the involvement of a possible feedback mechanism for the expression of TRIM proteins by interferon-mediated responses during viral infections. In summary, we suggest that JEV infection in human microglial cells triggers an innate immune response in terms of IFN-β production. The expression of IFN-β in turn is suppressed by increased expression of TRIM21 during JEV infection in human microglial cells. Probably JEV utilizes this strategy to suppress the type I interferon response as a part of an immune evasion mechanism. However, further studies are required to understand the involvement of other TRIM proteins as an antiviral factor against other flaviviruses in order to understand the mechanisms of pathogenesis as well as to develop therapeutic tools.

Conclusion

JEV infection in human microglial cells induced the expression of TRIM21 protein. Exogenous expression of TRIM21 in human microglial cells resulted in attenuation of JEV-mediated effects in terms of activation of interferon regulatory factor-3 and production of interferon-β. Further knockdown of TRIM21 enhances the JEV-mediated IRF-3 activation and IFN-β production. Although upstream mechanisms of JEV-mediated IRF-3 phosphorylation are known, this study provides the first evidence of the involvement of TRIM21 protein in negatively regulating the innate immune response by targeting IRF-3-mediated IFN-β production during JEV infection. JEV could exploit this strategy to suppress the type I interferon response during the early course of infection.

Additional file

Additional file 1: Figure S1. JEV infection does not affect TRIM21 protein levels in HeLa cells. HeLa cells were infected with JEV at MOI 5 and harvested at different time intervals of 6, 12, 24 and 36 h. Cells were either lysed for Western blotting against anti- TRIM21 antibody **(A)** or lysed using reporter lysis buffer for IFN-β luciferase assay **(B)**. All experiments were performed as sets of three independent experiments and data averaged and plotted as mean ± SEM (*$p < 0.05$, **$p < 0.01$, ***$p < 0.001$ from control, $^{\#}$p from 6 h, $^{\$}$p from 12 h).

Abbreviations

JEV: Japanese encephalitis virus; JE: Japanese encephalitis; PRR: Pattern recognition receptors; RLR: RIG-1 like receptors; RIG-1: Retinoic acid-inducible

gene 1; MDA5: Melanoma differentiation-associated protein 5; MAVS: Mitochondrial antiviral signaling protein; TLR: Toll-like receptors; TBK: Tank binding kinase; TGF: Transforming growth factor; IFN: Interferon; IRF: Interferon regulatory factor; TRIM: Tripartite motif; ISG: Interferon-stimulated genes; TAB2: TAK1 binding protein 2; TAB3: TAK1 binding protein 3; LPS: Lipopolysaccharide; MAPK: Mitogen-activated protein kinase; HSV: Herpes simplex virus.

Competing interests
The authors declare that they have no competing interests.

Authors' contributions
GDM designed the study, performed experiments and data analysis, and cowrote the manuscript. RM performed the PCR of the TRIM customized plate. NS carried out cloning work of TRIM21 and TRIM21 (ΔRING); KLM propagated the JEV in mice. AB provided the CHME3 cells and JEV as a kind gift. SKS conceived the idea, supervised the experiments and data analysis, and wrote the manuscript. All authors have read and approved the final version of the manuscript.

Acknowledgements
The authors are thankful to Prof. Adolfo Garcia-Sastre, Department of Medicine and Microbiology, Mount Sinai School of Medicine, NY, New York, USA, for providing the IFN-β-luciferase promoter as a kind gift. We are also thankful to Dr. Rajesh Singh, Associate Professor, Department of Biotechnology, MS University, Baroda, for useful discussions and support. The authors are also thankful to the director, Centre for Cellular and Molecular Biology (CCMB), Hyderabad, for his support. The financial support to GDM toward her postdoctoral fellowship through the CSIR network project (miND-BSC0115) is highly acknowledged. The authors acknowledge the financial support through the Indo-Korean Grant (INT/Korea/P-08) funded by the Department of Science and Technology, Government of India, New Delhi.

Author details
[1]Laboratory of Neurovirology and Inflammation Biology, CSIR-Centre for Cellular and Molecular Biology (CCMB), New R&D Building-1st Floor, Uppal Road, Hyderabad 500007, India. [2]National Brain Research Center (NBRC), Manesar, Haryana, India.

Received: 21 November 2013 Accepted: 19 January 2014
Published: 1 February 2014

References
1. Unni SK, Ruzek D, Chhatbar C, Mishra R, Johri MK, Singh SK: **Japanese encephalitis virus: from genome to infectome.** *Microbes Infect* 2011, **13:**312–321.
2. van den Hurk AF, Ritchie SA, Mackenzie JS: **Ecology and geographical expansion of Japanese encephalitis virus.** *Annu Rev Entomol* 2009, **54:**17–35.
3. Nazmi A, Dutta K, Basu A: **RIG-I mediates innate immune response in mouse neurons following Japanese encephalitis virus infection.** *PLoS One* 2011, **6:**e21761.
4. Lee MS, Kim YJ: **Pattern-recognition receptor signaling initiated from extracellular, membrane, and cytoplasmic space.** *Mol Cells* 2007, **23:**1–10.
5. Kato H, Takeuchi O, Sato S, Yoneyama M, Yamamoto M, Matsui K, Uematsu S, Jung A, Kawai T, Ishii KJ, *et al*: **Differential roles of MDA5 and RIG-I helicases in the recognition of RNA viruses.** *Nature* 2006, **441:**101–105.
6. Yoneyama M, Fujita T: **Structural mechanism of RNA recognition by the RIG-I-like receptors.** *Immunity* 2008, **29:**178–181.
7. Gitlin L, Barchet W, Gilfillan S, Cella M, Beutler B, Flavell RA, Diamond MS, Colonna M: **Essential role of mda-5 in type I IFN responses to polyriboinosinic: polyribocytidylic acid and encephalomyocarditis picornavirus.** *Proc Natl Acad Sci USA* 2006, **103:**8459–8464.
8. Kawai T, Sato S, Ishii KJ, Coban C, Hemmi H, Yamamoto M, Terai K, Matsuda M, Inoue J, Uematsu S, *et al*: **Interferon-alpha induction through Toll-like receptors involves a direct interaction of IRF7 with MyD88 and TRAF6.** *Nat Immunol* 2004, **5:**1061–1068.
9. Akira S, Uematsu S, Takeuchi O: **Pathogen recognition and innate immunity.** *Cell* 2006, **124:**783–801.
10. Peterson KE, Du M: **Innate immunity in the pathogenesis of polytropic retrovirus infection in the central nervous system.** *Immunol Res* 2009, **43:**149–159.
11. Fitzgerald KA, McWhirter SM, Faia KL, Rowe DC, Latz E, Golenbock DT, Coyle AJ, Liao SM, Maniatis T: **IKKepsilon and TBK1 are essential components of the IRF3 signaling pathway.** *Nat Immunol* 2003, **4:**491–496.
12. Sharma S, Benjamin R, Grandvaux N, Zhou GP, Lin R, Hiscott J: **Triggering the interferon antiviral response through an IKK-related pathway.** *Science* 2003, **300:**1148–1151.
13. McWhirter SM, Fitzgerald KA, Rosains J, Rowe DC, Golenbock DT, Maniatis T: **IFN-regulatory factor 3-dependent gene expression is defective in Tbk1-deficient mouse embryonic fibroblasts.** *Proc Natl Acad Sci USA* 2004, **101:**233–238.
14. Yoneyama M, Suhara W, Fukuhara Y, Fukuda M, Nishida E, Fujita T: **Direct triggering of the type I interferon system by virus infection: activation of a transcription factor complex containing IRF-3 and CBP/p300.** *Embo J* 1998, **17:**1087–1095.
15. McNab FW, Rajsbaum R, Stoye JP, O'Garra A: **Tripartite-motif proteins and innate immune regulation.** *Curr Opin Immunol* 2011, **23:**46–56.
16. Han K, Lou DI, Sawyer SL: **Identification of a genomic reservoir for new TRIM genes in primate genomes.** *PLoS Genet* 2011, **7:**e1002388.
17. Short KM, Cox TC: **Subclassification of the RBCC/TRIM superfamily reveals a novel motif necessary for microtubule binding.** *J Biol Chem* 2006, **281:**8970–8980.
18. Schwamborn JC, Berezikov E, Knoblich JA: **The TRIM-NHL protein TRIM32 activates microRNAs and prevents self-renewal in mouse neural progenitors.** *Cell* 2009, **136:**913–925.
19. Sato T, Okumura F, Kano S, Kondo T, Ariga T, Hatakeyama S: **TRIM32 promotes neural differentiation through retinoic acid receptor-mediated transcription.** *J Cell Sci* 2011, **124:**3492–3502.
20. Uchil PD, Hinz A, Siegel S, Coenen-Stass A, Pertel T, Luban J, Mothes W: **TRIM protein-mediated regulation of inflammatory and innate immune signaling and its association with antiretroviral activity.** *J Virol* 2011, **87:**257–272.
21. Stremlau M, Owens CM, Perron MJ, Kiessling M, Autissier P, Sodroski J: **The cytoplasmic body component TRIM5alpha restricts HIV-1 infection in Old World monkeys.** *Nature* 2004, **427:**848–853.
22. Yap MW, Nisole S, Lynch C, Stoye JP: **Trim5alpha protein restricts both HIV-1 and murine leukemia virus.** *Proc Natl Acad Sci USA* 2004, **101:**10786–10791.
23. Geoffroy MC, Chelbi-Alix MK: **Role of promyelocytic leukemia protein in host antiviral defense.** *J Interferon Cytokine Res* 2011, **31:**145–158.
24. Hattlmann CJ, Kelly JN, Barr SD: **TRIM22: a diverse and dynamic antiviral protein.** *Mol Biol Int* 2012, **2012:**153415.
25. Jefferies C, Wynne C, Higgs R: **Antiviral TRIMs: friend or foe in autoimmune and autoinflammatory disease?** *Nat Rev Immunol* 2011, **11:**617–625.
26. Higgs R, Ni Gabhann J, Ben Larbi N, Breen EP, Fitzgerald KA, Jefferies CA: **The E3 ubiquitin ligase Ro52 negzatively regulates IFN-beta production post-pathogen recognition by polyubiquitin-mediated degradation of IRF3.** *J Immunol* 2008, **181:**1780–1786.
27. Yang K, Shi HX, Liu XY, Shan YF, Wei B, Chen S, Wang C: **TRIM21 is essential to sustain IFN regulatory factor 3 activation during antiviral response.** *J Immunol* 2009, **182:**3782–3792.
28. Vaysburd M, Watkinson RE, Cooper H, Reed M, O'Connell K, Smith J, Cruickshanks J, James LC: **Intracellular antibody receptor TRIM21 prevents fatal viral infection.** *Proc Natl Acad Sci USA* 2013, **110:**12397–12401.
29. Bradford MM: **A rapid and sensitive method for the quantitation of microgram quantities of protein utilizing the principle of protein-dye binding.** *Anal Biochem* 1976, **72:**248–254.
30. Nazmi A, Mukhopadhyay R, Dutta K, Basu A: **STING mediates neuronal innate immune response following Japanese encephalitis virus infection.** *Sci Rep* 2012, **2:**347.
31. Ozato K, Shin DM, Chang TH, Morse HC 3rd: **TRIM family proteins and their emerging roles in innate immunity.** *Nat Rev Immunol* 2008, **8:**849–860.
32. Versteeg GA, Rajsbaum R, Sanchez-Aparicio MT, Maestre AM, Valdiviezo J, Shi M, Inn KS, Fernandez-Sesma A, Jung J, Garcia-Sastre A: **The E3-ligase TRIM family of proteins regulates signaling pathways triggered by innate immune pattern-recognition receptors.** *Immunity* 2013, **38:**384–398.
33. Taylor RT, Lubick KJ, Robertson SJ, Broughton JP, Bloom ME, Bresnahan WA, Best SM: **TRIM79alpha, an interferon-stimulated gene product, restricts tick-borne encephalitis virus replication by degrading the viral RNA polymerase.** *Cell Host Microbe* 2011, **10:**185–196.

34. Wang J, Liu B, Wang N, Lee YM, Liu C, Li K: **TRIM56 is a virus- and interferon-inducible E3 ubiquitin ligase that restricts pestivirus infection.** *J Virol* 2011, **85:**3733–3745.
35. McEwan WA, Tam JC, Watkinson RE, Bidgood SR, Mallery DL, James LC: **Intracellular antibody-bound pathogens stimulate immune signaling via the Fc receptor TRIM21.** *Nat Immunol* 2013, **14:**327–336.
36. Young JA, Sermwittayawong D, Kim HJ, Nandu S, An N, Erdjument-Bromage H, Tempst P, Coscoy L, Winoto A: **Fas-associated death domain (FADD) and the E3 ubiquitin-protein ligase TRIM21 interact to negatively regulate virus-induced interferon production.** *J Biol Chem* 2011, **286:**6521–6531.
37. Higgs R, Lazzari E, Wynne C, Ni Gabhann J, Espinosa A, Wahren-Herlenius M, Jefferies CA: **Self protection from anti-viral responses–Ro52 promotes degradation of the transcription factor IRF7 downstream of the viral Toll-like receptors.** *PLoS One* 2010, **5:**e11776.
38. Kong HJ, Anderson DE, Lee CH, Jang MK, Tamura T, Tailor P, Cho HK, Cheong J, Xiong H, Morse HC 3rd, Ozato K: **Cutting edge: autoantigen Ro52 is an interferon inducible E3 ligase that ubiquitinates IRF-8 and enhances cytokine expression in macrophages.** *J Immunol* 2007, **179:**26–30.
39. Zhang Z, Bao M, Lu N, Weng L, Yuan B, Liu YJ: **The E3 ubiquitin ligase TRIM21 negatively regulates the innate immune response to intracellular double-stranded DNA.** *Nat Immunol* 2013, **14:**172–178.
40. Shi M, Deng W, Bi E, Mao K, Ji Y, Lin G, Wu X, Tao Z, Li Z, Cai X, *et al*: **TRIM30 alpha negatively regulates TLR-mediated NF-kappa B activation by targeting TAB2 and TAB3 for degradation.** *Nat Immunol* 2008, **9:**369–377.
41. Zha J, Han KJ, Xu LG, He W, Zhou Q, Chen D, Zhai Z, Shu HB: **The Ret finger protein inhibits signaling mediated by the noncanonical and canonical IkappaB kinase family members.** *J Immunol* 2006, **176:**1072–1080.
42. Pertel T, Hausmann S, Morger D, Zuger S, Guerra J, Lascano J, Reinhard C, Santoni FA, Uchil PD, Chatel L, *et al*: **TRIM5 is an innate immune sensor for the retrovirus capsid lattice.** *Nature* 2011, **472:**361–365.
43. Tareen SU, Emerman M: **Human Trim5alpha has additional activities that are uncoupled from retroviral capsid recognition.** *Virology* 2011, **409:**113–120.
44. Li Q, Yan J, Mao AP, Li C, Ran Y, Shu HB, Wang YY: **Tripartite motif 8 (TRIM8) modulates TNFalpha- and IL-1beta-triggered NF-kappaB activation by targeting TAK1 for K63-linked polyubiquitination.** *Proc Natl Acad Sci USA* 2011, **108:**19341–19346.
45. Poole E, Groves I, MacDonald A, Pang Y, Alcami A, Sinclair J: **Identification of TRIM23 as a cofactor involved in the regulation of NF-kappaB by human cytomegalovirus.** *J Virol* 2009, **83:**3581–3590.
46. Sjostrand M, Ambrosi A, Brauner S, Sullivan J, Malin S, Kuchroo VK, Espinosa A, Wahren-Herlenius M: **Expression of the immune regulator tripartite-motif 21 is controlled by IFN regulatory factors.** *J Immunol* 2013, **191:**3753–3763.
47. Carthagena L, Bergamaschi A, Luna JM, David A, Uchil PD, Margottin-Goguet F, Mothes W, Hazan U, Transy C, Pancino G, Nisole S: **Human TRIM gene expression in response to interferons.** *PLoS One* 2009, **4:**e4894.
48. Rajsbaum R, Stoye JP, O'Garra A: **Type I interferon-dependent and -independent expression of tripartite motif proteins in immune cells.** *Eur J Immunol* 2008, **38:**619–630.
49. Chelbi-Alix MK, Pelicano L, Quignon F, Koken MH, Venturini L, Stadler M, Pavlovic J, Degos L, de The H: **Induction of the PML protein by interferons in normal and APL cells.** *Leukemia* 1995, **9:**2027–2033.
50. Asaoka K, Ikeda K, Hishinuma T, Horie-Inoue K, Takeda S, Inoue S: **A retrovirus restriction factor TRIM5alpha is transcriptionally regulated by interferons.** *Biochem Biophys Res Commun* 2005, **338:**1950–1956.
51. Strandberg L, Ambrosi A, Espinosa A, Ottosson L, Eloranta ML, Zhou W, Elfving A, Greenfield E, Kuchroo VK, Wahren-Herlenius M: **Interferon-alpha induces up-regulation and nuclear translocation of the Ro52 autoantigen as detected by a panel of novel Ro52-specific monoclonal antibodies.** *J Clin Immunol* 2008, **28:**220–231.
52. Zhao W, Wang L, Zhang M, Yuan C, Gao C: **E3 ubiquitin ligase tripartite motif 38 negatively regulates TLR-mediated immune responses by proteasomal degradation of TNF receptor-associated factor 6 in macrophages.** *J Immunol* 2012, **188:**2567–2574.

doi:10.1186/1742-2094-11-24
Cite this article as: Manocha *et al.*: Regulatory role of TRIM21 in the type-I interferon pathway in Japanese encephalitis virus-infected human microglial cells. *Journal of Neuroinflammation* 2014 **11**:24.